Energy Conversion and Management 276 (2023) 116569

Contents lists available at ScienceDirect

Energy Conversion and Management

journal homepage: www.elsevier.com/locate/enconman

Development of a hybrid biorefinery for jet biofuel production

Mohammad Alherbawi, Gordon McKay, Tareq Al-Ansari *

Division of Sustainable Development, College of Science and Engineering, Hamad Bin Khalifa University, Qatar Foundation, Doha, Qatar

A R T I C L E I N F O

Keywords:
Jet biofuel
Hybrid biorefinery
Waste-to-Energy
Qatar
Aspen Plus
GIS

A B S T R A C T

Jet biofuel (JBF) is identified as an essential solution to mitigate the carbon footprint of the aviation sector. Since aeroplanes rely solely on liquid fuels, the development of pathways that generates JBF as a major product has become crucial. Thus far, seven pathways to produce JBF have been developed and certified over the past decade. Each of these pathways accommodates a specific type of biomass. However, the availability, sustainability and feasibility of feedstocks to fulfil the growing demand on jet fuel remains an issue. As such, this study presents a holistic approach for the design of a state-of-the-art hybrid biorefinery that accommodates multiple biomass feedstocks across different categories including energy crops (i.e., *Jatropha* energy crop), dry biomass (i.e., municipal solid waste) and wet biomass (i.e., livestock manure). A Qatar-based industrial scale biorefinery was modelled in Aspen Plus® considering a pre-defined geospatial distribution of biomass and the optimal biorefinery site in the country. The hybrid system integrated advanced technologies such as hydroprocessing, Fischer-Tropsch, gasification, dry-reforming and hydrothermal liquefaction. While biomass optimal insertion streams were evaluated using a prediction model. Besides, intensive materials, heat, water and power integrations were performed to maximise JBF production, mitigate its environmental impact and control its cost. The system generated 328, 94 and 44 million litres of JBF, gasoline and diesel, respectively. Produced JBF was characterised and found to comply with all international standards. The generated JBF can substitute 15.3 % of Qatar's jet fuel needs, while it can power around one third of its fleet considering a maximum allowable jet biofuel blend of 50 %. The proposed model achieved a minimum selling price of JBF at 0.43 $/kg, which is 22 % lower than the market price of conventional Jet-A fuel (2019). In addition, the environmental analysis of the model indicated a 41 % mitigation in greenhouse gas emissions achieved by JBF throughout its lifecycle, relative to Jet-A fuel.

1. Introduction

Biomass-to-energy technologies occupy ~ 70 % of the gross global renewables [1], which is gradually increasing in parallel with the rise of demand on energy resources and fossil fuels' price fluctuation due to global political and economic instability.

Recent decades have witnessed a great development of technologies that accommodate different biomass types; including anaerobic digestion to process putrescibles, fermentation of sugar-based feedstocks, pyrolysis and gasification of dry solid biomass, hydrothermal liquefaction (HTL) to liquify wet biomass, and incineration for a direct conversion of biomass into energy [2]. While intermediate products of these processes including syngas, biomethane, bioethanol and biocrude have been upgraded into liquid transportation fuels through well-established technologies like the hydroprocess and the Fischer-Tropsch (FT) process. However, as far as the air transportation sector is concerned, the only viable alternative fuel to be currently considered shall be a drop-in liquid fuel with high quality and considerable energy density to avoid the costly modifications of turbine jet engines.

In this context, the International Civil Aviation Organisation (ICAO) has launched an initiative called "Carbon Offsetting and Reduction Scheme for International Aviation (CORSIA)" in 2016, which targets offsetting all additional emissions above the 2019–2020 baseline [3]. Where jet biofuel (JBF) has been considered to be the key alternative to fulfil the ambitious plan of the international aviation industry. While growing carbon neutral energy crops is identified as the principal mean to achieve CORSIA goals.

JBF (also called aviation bio-kerosene) is a group of paraffins that correspond to the kerosene boiling point range, fall within hydrocarbon lengths of (C8-C16) and comply to most of fossil jet fuel standard properties. It can be generated from wide range of renewable biomass including oil triglycerides, sugar, and lignocellulosic wastes [4].

* Corresponding author.
E-mail address: talansari@hbku.edu.qa (T. Al-Ansari).

https://doi.org/10.1016/j.enconman.2022.116569
Received 12 October 2022; Received in revised form 27 November 2022; Accepted 10 December 2022
Available online 20 December 2022

Meanwhile, seven production pathways at least have been certified for different types of feedstocks by the American Society for Testing and Materials (ASTM). These pathways include: hydroprocessing of esters and fatty acids (HEFA), Fischer-Tropsch synthetic paraffinic kerosene (FT-SPK), Fischer-Tropsch synthetic paraffinic kerosene with aromatics (FT-SPK/A), hydroprocessing of fermented sugars - synthetic iso-paraffinic kerosene (HFS-SIP), alcohol-to-jet synthetic paraffinic kerosene (ATJ-SPK), catalytic hydrothermolysis to jet (CHJ), and synthetic paraffinic kerosene from hydrocarbon-hydroprocessed esters and fatty acids (HC-HEFA-SPK) using microalgae [5]. The permissible blending ratios of these fuels do not exceed 50 % as they mostly lack some essential components of conventional jet fuel such as aromatics or iso-paraffins. In addition, these pathways are capable to accommodate only a single category of feedstock (either lipid, sugar, alcohol or solid biomass), while the fuel price they offer is still beyond the competition with the existing conventional fuels [6]. As such, development of integrated pathways may overcome the drawbacks of individual pathways, and maximise yield and returns [7].

There are limited reports on the development of integrated technologies that combines multiple processes to produce JBF from biomass. Sadhukhan and Sen [8] presented a pyrolysis-based integrated biorefinery for jet biofuel production. The proposed system upgrades bio-oil into liquid transportation fuel via hydroprocessing, while steam reforming and pressure swing adsorption are employed to generate hydrogen, along with on-site power generation. Besides, Kumar et al. [9] suggested multiple products generation out of sugarcane; including JBF and ethanol. The former system attained a minimum selling price (MSP) of JBF at 0.6–1.4 $/kg for a refinery feed capacity of 1.6 Mtonnes/y. Likewise, Santos et al. [10], studied 81 integration scenarios of JBF production in a Brazilian sugarcane biorefinery, with the lowest MSP of 1.69 $/kg achieved through sugar conversion via alcohol-to-jet pathway, and bagasse to JBF through fast pyrolysis and upgrading.

Wang [11] made use of the *Jatropha* shells and seedcake to generate electricity and pyrolysis oil, along with the upgrading of *Jatropha* oil into JBF. The former system scored a 6 % reduction in JBF cost relative to valorising the fruit's oil only. Similarly, Romero-Izquierdo et al. [12] evaluated the processing of castor bean fruit into multiple products including JBF, bio-oil and biochar. Whereas Tanzil et al. [13] evaluated multiple integrated scenarios based on existing sugarcane mill facilities, achieving MSP reduction of up to 53 % (at ~ 1.3 $/kg). Furthermore, Alherbawi et al. [14] proposed an integrated pathway to utilise whole *Jatropha* energy crop through the integration of HEFA and FT-SPK pathways, achieving a jet biofuel's MSP of 0.45–0.99 $/kg. Besides, Julio et al. [15] proposed an integration of alcohol-to-jet process into existing palm oil biorefineries for the production of JBF from a second generation biomass, achieving an MSP of 0.58 $/kg. Nevertheless, Romero-Izquierdo et al. [16] proposed a biorefinery design based on simultaneous production of biodiesel and JBF using waste cooking oil via esterification and hydrotreatment processes, with an MSP of JBF at 0.74 $/kg. Meanwhile, several studies have investigated the co-processing of renewable feeds in conventional refineries [17].

However, no JBF biorefinery design is reported, in which multiple feedstocks across different biomass categories are accommodated, which requires high level of integration and involvement of various technologies. Integrated biorefineries provides the chance for by-products conversion into higher value products, process' waste valorisation, and enhancement of the refinery economics [18]. The design of such hybrid biorefinery is challenging due to feedstock diversity, heterogenous nature and seasonal variation [19,20]. Budzianowski and Postawa [21] concluded that a robust integrated biorefinery design requires applying efficient conversion pathways, optimising the biomass supply chain, enlarging feedstock base and exchanging wastes and by-products with other systems. Whereas Özdenkçi et al. [22] stated that strategic decisions to define optimal supply chain for biorefineries may include selection and definition of biomass types, availability, supplying sites and their corresponding conversion technologies.

Therefore, this study and its previously published parts present a holistic approach for the design of a novel hybrid biorefinery to utilise multiple biomass in the State of Qatar. Earlier, a databank on the geo-spatial distribution of biomass in Qatar has been created in ArcGIS, while the optimal site to establish the biorefinery was selected based on multiple criteria using the maximal coverage location algorithm to enhance the biomass supply chain [23]. Moreover, a regression predictive model was then developed through intensive simulations to provide a mathematical formulation for the selection of optimal processing pathway for each biomass category, this predictive model enabled the selection of biomass insertion stream into the hybrid biorefinery [24]. In this study, a hybrid biorefinery was developed in Aspen Plus to produce JBF as the key product using multiple feeds across different biomass categories (i.e., *Jatropha* energy crop, livestock manures, and MSW). The model comprises key advanced processes including hydroprocessing, FT, reforming, gasification, and HTL. Intensive integration of streams was performed to maximise JBF, minimise solid and gaseous by-products, and recycle process' wastes. In addition, the biorefinery economics was evaluated, while its environmental lifecycle performance was investigated from cradle to grave.

2. Methodology

2.1. Hybrid biorefinery design

Aspen Plus (V.10) ® was employed to design the hybrid biorefinery for the production of JBF using multiple biomass sources in Qatar. The system mainly integrates two ASTM-certified JBF pathways: the hydroprocessing of triglycerides, and biomass gasification, followed by FT. Besides, a third route comprises HTL and upgrading was integrated with the system, while a dry-reforming stage (using CO_2) was employed to enhance JBF yield and to reduce the refinery's carbon footprint. The system was designed to accommodate almost all types of local biomass including *Jatropha curcas* whole-fruit, dry and wet solid wastes in a single biorefinery; while the process runs on jet-mode to maximise JBF yield. The biorefinery flowsheet is presented in Fig. 1.

The system was modelled considering the assumptions of an isothermal system and steady-state reactions. The Redlich-Kwong-Soave (RK-SOAVE) and the non-random two-liquid model (NRTL) models were used for the estimation of the thermodynamic properties. Different integration and intensification techniques were employed within the system including heat, water and power integration, as well as waste valorisation, carbon capture and storage. The model offers a great extent of by-products utilisation within the system, to end up with green liquid fuels only at boosted quantities. In addition, the system was designed to be utility-self-sufficient, whereby power and water are produced on-site. The following subsections detail out the design of each sub-system.

2.1.1. Upstream stage

Three categories of biomass were selected to be utilised in the proposed system, including *Jatropha curcas* energy crop, municipal solid waste (MSW), and livestock manures. These feedstocks have been identified using a predictive model that was established earlier by the authors [24], whereby MSW was identified to be processed through the gasification pathway, while livestock manures were identified for HTL pathway. *Jatropha* was selected due to its high potential to grow in Qatar with minimal water and energy requirement, while MSW and livestock manure of different types were selected due to their wide availability in the country to represent low-moisture and high-moisture biomass, respectively.

The quantity of *Jatropha* fruits was defined based on the delineated *Jatropha*-greenbelt in author's earlier study [25]. It was assumed that the greenbelt is of 227 km length and 2 km width.

Great differences in *Jatropha* seed productivity have been stated from as low as 0.1 up to 15 tonne/ha annually [26]. The variation is due to different growing conditions, as well as the different reported stage of

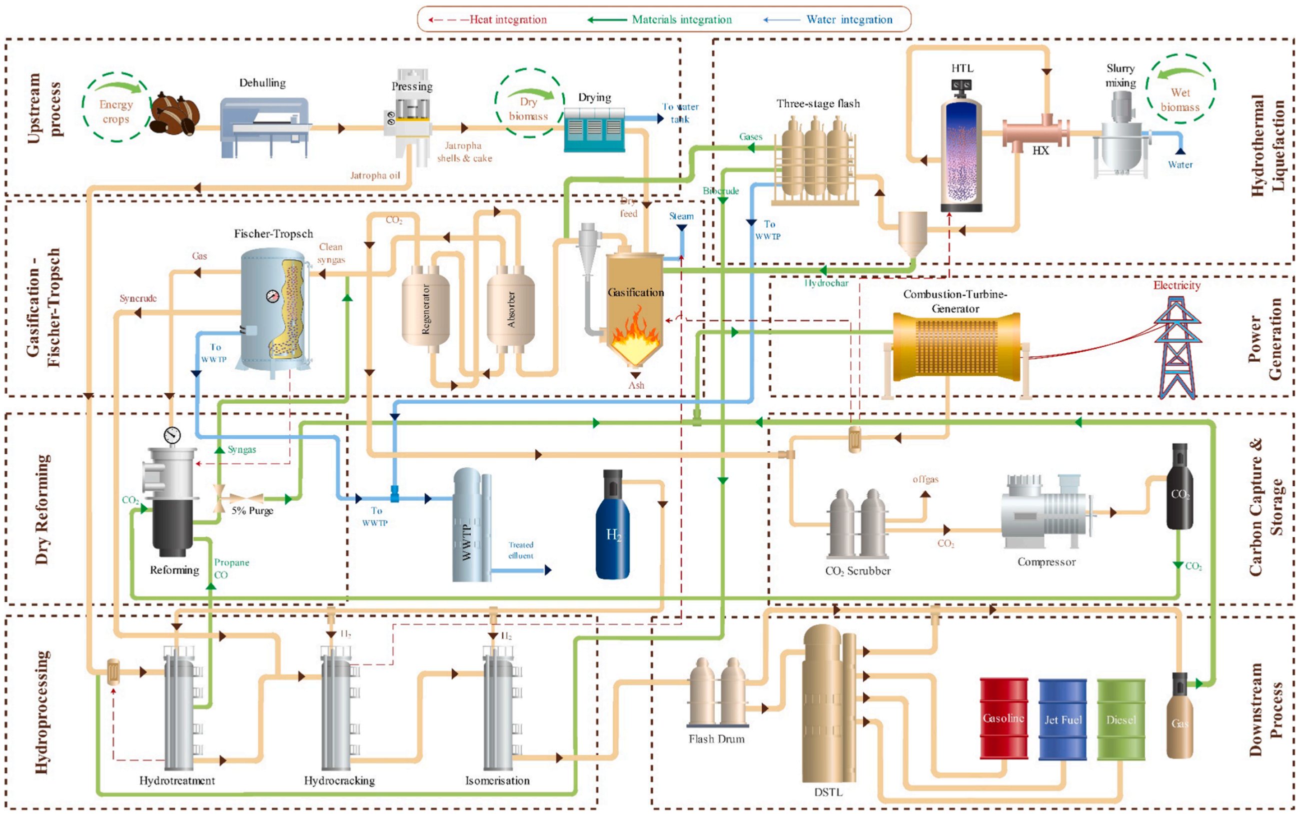

Fig. 1. Flowsheet of the developed hybrid biorefinery.

cultivation; where in early years, *Jatropha* yields minimal quantity, reaching the peak by the 3rd to 5th year [27]. However, when the whole fruit is considered, the biomass yield could reach to 20 tonne/ha considering a fruit shell composition of 30 wt% of the fruit [28]. Therefore, an average of 10 tonne/ha yield of mature crop was considered in this study, which complies with published reports [29,30].

Initially, all solid feeds were defined in Aspen Plus as non-conventional components using their elemental and proximate characteristics presented in Table 1. While the *Jatropha* oil was assumed to be 25 wt% of the *Jatropha* fruit (oil flow: 136,200 t/y), and defined based on its triglycerides composition listed in Table 1 [31]. The *Jatropha* fruits were first put through a machine-driven dehuller to separate the fruit shells, and the seeds were then processed in a pressor to obtain the oil. The resulting components were determined considering the given fruit composition, while the power needs for both machines were evaluated based on similar industrial machines [11].

Upon dehulling and pressing, three effluent streams were obtained; the oil was fed into the hydrotreatment unit, whereas the fruit shells and seedcake were dried along with selected local dry municipal solid wastes (MSW) and HTL's hydrochar before being introduced into the gasifier. A rotary dryer was simulated using an "RYield" block and operated at 110 °C. The products of the drying stage were determined considering the feeds proximate analysis, where the dried residues were re-defined with a zero-moisture content. The moisture effluent was condensed and collected in a water storage tank.

2.1.2. Hydrothermal liquefaction

The wet biomass feeds were initially introduced into a blending

Table 1
Proximate and elemental analysis of solid biomass used in this study.

Characteristics	Wet waste					Dry waste	Energy crop	
Analysis [a]	Camel manure	Dairy manure	Horse manure	Poultry manure	Sheep manure	MSW	Seed-cake	Fruit shells
Flow (1000 tonne/year)	120	205.5	8.03	271.2	83.44	530	158.9	158.9
Moisture (%)[b]	58	85	40	40	50	7.56	4.08	10.57
Fixed carbon (%)[c]	22.7	10.1	12.1	13.3	15.6	24.21	19.06	17.64
Volatile matter (%)[c]	60.5	57.2	77.8	63.6	57.3	57.99	73.70	71.52
Ash (%)[c]	16.7	32.7	10.1	23.1	27.1	17.8	7.24	10.84
Carbon (%)[c]	37.1	27.6	39.5	36.7	33.1	48.23	52.12	40.8
Hydrogen (%)[c]	4.1	3.5	5.0	5.3	4.5	5.16	6.91	5.90
Nitrogen (%)[c]	2.3	1.9	0.7	3.5	2.7	1.21	5.01	1.53
Sulphur (%)[c]	0.2	0.4	0.5	0.7	0.4	0.29	0.70	0.43
Oxygen (%)[c]	39.5	33.9	44.2	30.6	32.2	27.31	28.02	40.5
Jatropha lipid profile (%)[d]: LLL: 5.03, OLL: 22.59, POL: 8.21, PLL: 25.47, OOL: 23.11, PPL: 1.54, OOO: 8.04, POP: 2.14, PPP: 2.91, SOO: 0.85, POS: 0.11								

a) Analysis are adapted from literature [31–38] b) evaluated on wet basis, c) normalised on dry basis.
d) L: Linoleic acid, O: Oleic acid, P: palmitic acid, S: Stearic acid.

unit, where they were transformed using a Fortran code into conventional components depending on their proximate and elemental characteristics to achieve a mass balance of the conversion [39]. A hydrolysis reactor was then supplied with the blended stream and additive water to produce a slurry. A Fortran code was created to calculate the quantity of water needed to dilute the solids concentration in the slurry to 20 % based on Equation (1). The key HTL reactions were carried out at 100 bar and 300 °C after the mixture was pumped to 100 bar using two successive high-pressure pumps.

At this stage, the highest possible biocrude and the lowest possible hydrochar generation were regulated using a Fortran code considering correlations adapted from Zhong and Wei [40] and Demirbaş [41] as presented in Equations (2) and (3), respectively. Meanwhile, the composition of crude and char were adapted from Magdeldin et al. [42] and Lentz et al. [43], respectively. A second HTL unit was designed to evaluate the final yields and compositions of biocrude and syngas via the minimisation of Gibb's free energy approach.

$$Additivewater = \left(\frac{dryfeed}{0.2}\right) - wetfeed \tag{1}$$

$$\text{Char Yield} = \sum_{i=1}^{5}\left(\left(\left(0.0608^{*}FC_i^2\right) - \left(1.7057^{*}FC_i\right) + 21.7539\right)^{*}\frac{100 - moist_i}{10000}{*}\text{FLOWi}\right)\Big/\text{TotalSlurry} \tag{2}$$

$$\text{Biocrude Yield} = \sum_{i=1}^{5}\left(\left(\left(0.03545^{*}FC_i^2\right) + \left(0.99^{*}FC_i\right) + 24.65\right)^{*}\frac{100 - moist_i}{10000}{*}\text{FLOWi}\right)\Big/\text{TotalSlurry} \tag{3}$$

Where, "i" represents different manure types. (1–5), FC_i: fixed carbon of manure "i", $FLOW_i$: input stream of manure "i".

In order to recover heat, the HTL intermediate product stream was fed into a heat exchanger before proceeding to the next stage of the process. Solids were removed using a solid separator and sent to the gasification section, while the volatile stream was divided into gaseous, aqueous, and biocrude oil phases by a three-stage flash unit. The biocrude was routed to the hydrotreatment unit, and the gas phase was handled in gas cleaning units. Finally, the aqueous phase was pumped to an on-site wastewater treatment unit.

2.1.3. Steam gasification

An entrained flow gasifier was applied in this study using steam as a gasifying agent [44]. The reactions were conducted at 1100 °C and a steam to feed ratio of 0.5 [45]. Decomposition was the first step in breaking down biomass to simpler components. To satisfy Equation (4), the process was simulated using two successive units. The first unit was represented by an "RYield" block, whereby unconventional components (i.e., hydrochar and dry biomass) were converted into conventional components including char, solid sulphur, hydrogen, nitrogen and oxygen. The conversion was conducted using a Fortran code to ensure an accurate mass balance [45]. The second unit using an "RGibbs" block was designed to convert volatile carbon into possible products (i.e., methane, carbon dioxide, carbon monoxide), while nitrogen and sulphur contents were transformed into ammonia and hydrogen sulphide, respectively, due to the significant presence of hydrogen in the reaction medium.

Oxidation processes occurred in the next stage due to the presence of oxygen as an intermediate product of the breakdown stage at a high operating temperature. Key reactions were simulated considering Equations 5–8 using an "REquil" unit. The last phase of the gasification reactions was modelled using a "RGibbs" block, which calculates phase and chemical equilibrium by minimising the Gibbs free energy. The resulting gases throughout these stages comprised H_2, CO, CO_2, H_2O, CH_4, NH_3 and H_2S as presented in Equations 9–13. However, almost all char content was anticipated to be volatilized by the end of the reaction, while ash is discharged as waste at the end of the process. The reactions in Equations 4–13 were assumed to be the only processes happening at the given conditions to ensure model simplicity.

$$\text{Pyrolysis: Biomass} \rightarrow \text{Char} + \text{Tar} + NH_3 + H_2S + H_2 + CO + CO_2 \tag{4}$$

$$\text{Complete char combustion: } C + O_2 \longleftrightarrow CO_2 \tag{5}$$

$$\text{Incomplete char combustion: } C + ½\, O_2 \longleftrightarrow CO \tag{6}$$

$$\text{Steam production: } H_2 + ½\, O_2 \longleftrightarrow H_2O \tag{7}$$

$$\text{CO oxidation: } CO + ½\, O_2 \longleftrightarrow\longleftrightarrow CO_2 \tag{8}$$

$$\text{Boudouard reaction: } C + CO_2 \longleftrightarrow 2CO \tag{9}$$

$$\text{Methanation: } C + 2H_2 \longleftrightarrow CH_4 \tag{10}$$

$$\text{Steam gasification: } C + H_2O \longleftrightarrow CO + H_2 \tag{11}$$

$$\text{Methane reforming: } CH_4 + H_2O \longleftrightarrow CO + 3H_2 \tag{12}$$

$$\text{Water gas shift reaction: } CO + H_2O \longleftrightarrow CO_2 + H_2 \tag{13}$$

A two-phase flash separator was employed to dry the wet syngas. The optimal operating conditions of the flash unit were evaluated based on automated sensitivity analysis, where it was run at a high pressure of 40 bar. Water was processed into an on-site wastewater treatment unit before collection in a water storage tank. Wax was condensed and transferred to hydrotreatment unit, while syngas was stripped of impurities (mainly CO_2, NH_3 and H_2S) using the methanol absorption system [14], where impurities were dissolved into chilled methanol at a high pressure.

2.1.4. Fischer-Tropsch

The FT reactions comprise two key phases: Initially the feed is broken down into simple monomers, then polymerisation takes place to form longer molecules [46]. A cobalt-based catalyst is often used to catalyse the process as it preserves high stability [47].

The slurry-phase reactor (SPR) was selected to conduct FT process, which was catalysed by Co/Al_2O_3 at a gas hourly space velocity of 2.38 m^3/hr.kg [48]. The FT simulation started with pumping the purified syngas into the FT reactor represented by "RYield" block. The process was conducted at 240 °C and 25 bar, where the possible products distribution was calculated using a Fortran code considering the Anderson-Schulz-Flory (ASF) correlation [49]:

$$F_n = n(1-\alpha)^2\alpha^{(n-1)} \tag{14}$$

Where; F_n: mass fraction of compounds of (n) carbons, n: length of the carbon chain, and ά: possibility of appearance (0 < ά < 1).

In order to achieve highest possibility of kerosene-range compounds to occur, ά value was fixed at 0.85. CO conversion percentage of 80 % into paraffins, olefins, and alcohols was considered [50]. Therefore, nearly 50 chemical reactions equations were plugged in, accounting for the pathways leading to the occurrence of predicted hydrocarbons as illustrated in Table A1. Meanwhile, the FT operating conditions that corresponds to the ά value of 0.85 for cobalt-catalysed process were defined based on alpha correlation introduced by Song et al. [51]:

$$\alpha_{ASF} = \left[0.2332\frac{x_{CO}}{x_{H_2} + x_{CO}} + 0.663\right][1 - 0.0039(T - 533)] \tag{15}$$

Where, X_{CO} and X_{H2} are molar fractions of CO and H_2 in the feed gas, respectively. T: is the operating temperature in kelvin.

The FT effluent was then passed through a multi-stage flash drum, where condensed moisture was removed and processed into the on-site wastewater treatment unit. In addition, generated gases (i.e., methane, ethane and propane) were fed in a dry-reforming reactor, whereas higher hydrocarbons were fractionated in a distillation unit, where wax was removed and sent to the hydrocracker and the simpler compounds are passed to the final distillation unit.

2.1.5. Dry reforming

The reforming process can be conducted using steam (wet reforming) or carbon dioxide (dry reforming) as reforming agents [52]. Wet reforming produces syngas with higher H_2:CO ratio than dry reforming, however, dry reforming is seen to be more environmentally friendly [53]. In this model, the dry-reforming process was integrated within the biorefinery to boost fuel production and mitigate the produced carbon dioxide. The process was simulated at 800 °C, and CO_2/CH_4 ratio of 5 using Ni/Al_2O_3 catalyst at a gas hourly space velocity of 327 L/hr.g. Dry reforming is an extremely endothermic process, requiring a high quantity of heat to drive the reaction forward. In contrast, FT is extremely exothermic. As such, based on initial energy analysis, the heat released by FT was roughly equal to the heat needed by the reforming unit, therefore, heat integration between the two units was performed to reduce overall energy requirement. An “RStoic” block was used to simulate the process, in which the possible following reactions were defined, with a fractional conversion of 95 % [53,54]:

$$C_nH_{(2n+2)} + nCO_2 \longleftrightarrow 2nCO + (n + 1)H_2 \tag{16}$$

2.1.6. Hydrotreatment

When the oil’s triglycerides were subjected to hydrotreatment, they break into propane and fatty acids as expressed by Equation (17). Propane was fed into the reforming section, and fatty acids were then saturated during the process, while their oxygen content was omitted via deoxygenation [55]. As for biocrude and wax feed, the hydrotreatment is meant to eliminate their heteroatoms contents (O, N and S) and saturate the double bonds. Hydrotreatment was run at operating temperature range of (300–400 °C), while the vessel pressure is highly governed by the feed composition, whereby it varies from as low as 30 bar for triglycerides, up to 120 bar for biocrude and bio-oil. As such, the hydrotreatment was conducted in two parallel reactors to accommodate both, the *Jatropha* oil and biocrude separately for a better control of the outputs.

Two blocks were simulated to represent the two key stages of *Jatropha* oil hydrotreatment (hydrogenation and deoxygenation). Both stages were run at 300 °C and 45 bar and a hydrogen supply ratio of around 1 wt%. Nickel-based catalyst was employed at a liquid hourly space velocity of 2 kg/hr.kg [56]. To compute phase and chemical equilibrium, the hydrogenation reaction was simulated using a “RGibbs” block. Based on the hydrogenation reactions shown in Equations 18–20, probable products may include different fatty acids and propane. However, the “REquil” unit was used to simulate deoxygenation reactions. Deoxygenation, decarboxylation, and decarbonylation were the key pathways for the omitting of oxygen, resulting in the release of H_2O, CO_2, and CO, respectively. The possible chemical pathways for this phase are shown in Equations 21–29. Given the operating conditions, marginal cracking occurred at this process [57,58]. The effluent of this process mainly included $C_{15}H_{32}$, $C_{16}H_{34}$, $C_{17}H_{36}$ and $C_{18}H_{38}$, in addition to minimal amounts of olefines and fatty acids.

Propane cleavage:

$$\text{Triglyceride} + 3\ \text{H2} \rightarrow 3\ \text{Fatty acid} + \text{Propane} \tag{17}$$

Hydrogenation:

$$C_{18}H_{32}O_2 + H_2 \rightarrow C_{18}H_{34}O_2 \tag{18}$$

$$C_{18}H_{32}O_2 + 2\ H_2 \rightarrow C_{18}H_{36}O_2 \tag{19}$$

$$C_{18}H_{34}O_2 + H_2 \rightarrow C_{18}H_{36}O_2 \tag{20}$$

Deoxygenation:

$$C_{18}H_{36}O_2 + 3\ H_2 \rightarrow C_{18}H_{38} + 2\ H_2O \tag{21}$$

$$C_{16}H_{32}O_2 + 3\ H_2 \rightarrow C_{16}H_{34} + 2\ H_2O \tag{22}$$

$$C_{18}H_{34}O_2 + 3\ H_2 \rightarrow C_{18}H_{36} + 2\ H_2O \tag{23}$$

Decarboxylation:

$$C_{18}H_{36}O_2 \rightarrow C_{17}H_{36} + CO_2 \tag{24}$$

$$C_{16}H_{32}O_2 \rightarrow\rightarrow C_{15}H_{32} + CO_2 \tag{25}$$

$$C_{18}H_{34}O_2 \rightarrow C_{17}H_{34} + CO_2 \tag{26}$$

Decarbonylation:

$$C_{18}H_{36}O_2 + H_2 \rightarrow C_{17}H_{36} + CO + H_2O \tag{27}$$

$$C_{16}H_{32}O_2 + H_2 \rightarrow C_{15}H_{32} + CO + H_2O \tag{28}$$

$$C_{18}H_{34}O_2 + H_2 \rightarrow C_{17}H_{34} + CO + H_2O \tag{29}$$

For biocrude and wax stream, one unit of “RGibbs” was considered to simulate the hydrotreatment reactions using nickel-based catalyst at 2 kg/hr.kg [56]. The process was conducted at 300 °C and 110 bar; while hydrogen was supplied at 0.03 kg/kg of feed. A limited hydrogen supply is meant to enhance aromatics preservation, which are an important component of jet fuel. Like the other hydrotreatment unit, the biocrude content of oxygen was removed through the formerly mentioned deoxygenation pathways, releasing H_2O, CO and CO_2; whereas nitrogen and sulphur compositions are transformed into ammonia and hydrogen sulphide, respectively. The possible predicted refined components of biocrude were define based on previous work, as presented in Table A2.

The effluent stream was then fed into a multi-stage flash drum to obtain three phases of upgraded fuels, gas and an aqueous phase. The upgraded oil was sent to the cracking unit, while the useful gas obtained from all hydrotreatment units (i.e., H_2O, CO_2, CO, H_2, C_2H_6, and CH_4) were cleaned along with the crude syngas, and further processed into FT and reforming units that are elaborated in the previous sections.

2.1.7. Hydrocracking and isomerisation

To maximise JBF selectivity, the obtained hydrocarbons must mostly be in the C8-C16 range. Therefore, waxes and long chain paraffins were subjected to cracking. Hydrocracking frequently necessitates higher pressures and temperatures than hydrotreatment [6], while JBF selectivity rises with increasing operating pressure [59]. In this model, the hydrocracking reactions were carried out at 350 °C and 80 bar, using zeolite catalyst at 1.84 kg/hr.kg [60,61]. Where the effluent streams of FT and hydrotreatment units were merged and pumped into the cracking reactor. Predicted cracked compounds were pre-defined comprising all straight and branched paraffins (C1-C20), as well as expected traces of oxygenated hydrocarbons.

In addition, isomerisation of the product is needed to improve JBF quality [62], as branched paraffins exhibit lower freezing point and surface tension [63]. Therefore, isomerisation process was conducted separately to have a better control over the products characteristics. The products distributions of the process were defined based on an experimental study using platinum-alumina catalyst system as illustrated in Table A3 [64]. The process was conducted at 180 °C and 20 bar in “RStoic” block [65].

2.1.8. Downstream process

A merged stream obtained from the multiple integrated pathways was pumped through subsequent down-streaming units to obtain various fuel categories. The stream was firstly processed into a multi-stage flash drum at 60 °C and 20 bar to ensure the removal of water and for initial gas–liquid separation. Higher hydrocarbons were then fed into a fractionation column with 18 stages, to collect different fuel cuts including JBF, gasoline and diesel. Whereas the collected fuel gas was utilised for power generation to run the biorefinery.

2.1.9. Power generation and heat integration

Prior to the injection of reformed gas into the FT section, nearly 5 wt % of the gas was diverted to preserve the cycle at an appropriate pressure level. The diverted gas portion is processed along with distilled gas product at a gas-turbine to generate power. A General Electric (GE) power generator of 53 % efficiency was considered for an on-site electricity generation. Based on the input gases, all the combustion pathways were determined using an "RStoic" unit with sufficient air supply to guarantee a perfect combustion. The high-pressure effluent runs across the GE turbine to produce the needed electricity [39]. In addition, the heat produced through the different exothermic reactions (i.e., FT, cracking, etc.) was valorised in providing the required heat supply for the endothermic reactions such as reforming and liquefaction. While heat exchangers were plugged into the refinery to further valorise heat within the subsystems.

2.1.10. Carbon capture and wastewater treatment units

To further enhance the environmental performance of the developed biorefinery, a carbon capture and storage (CCS), and a wastewater treatment plant (WWTP) were added to the system.

The flue gas exiting the gas turbine was collected and fed into a methanol-based carbon capture unit. A cool methanol solvent (-60 °C) was utilised to capture carbon dioxide, which occurred in different gas streams throughout the various processes. Methanol was passed at high pressure through an absorption column against the gas stream, where CO_2 was dissolved in methanol and transferred to the scrubber unit, in which CO_2 was scrubbed at low pressure and sent to a compressor unit along with CO_2 captured in the syngas cleaning unit. Part of the carbon dioxide was utilised in the dry reforming, while the excess CO_2 was compressed at 50 bar and stored in high-pressure gas vessels. Furthermore, fractional distillation was employed to treat the process' wastewater to a permissible level for use in industry or agriculture. Whereby, a "RadFrac" distillation column with a 16-stage process was used at a reflux ratio of 1. Treated water was evaluated in terms of chemical oxygen demand (COD) and collected in a water storage tank.

2.1.11. Process integration and intensification

Intensive integration of streams amongst the different sub-systems was performed to maximise the JBF yield at the expense of other fuel categories and to enhance the system's economics and environmental performance, as follows:

i. Hydrotreatment's gases including carbon monoxide, carbon dioxide, propane, and excess hydrogen were integrated with the crude syngas stream to enhance hydrogen to carbon ratio and to valorise these gases.
ii. HTL's gas phase was merged with the crude syngas stream to recover carbon dioxide and enhance the net clean syngas yield.
iii. FT gas products were integrated into the dry reforming section to enhance syngas feed into FT reactor, and therefore boost the liquid fuels yield.
iv. HTL's hydrochar product stream is integrated with the gasification section to convert all solid products to volatile fuels.
v. Gasification's tar product was fed into the hydrotreatment and hydrocracking sections for upgrading purpose.
vi. FT's wax products were transferred to the hydrocracking section to break them down to shorter hydrocarbons that correspond to liquid transportation fuels.
vii. Captured CO_2 was supplied to the dry-reforming section as a reforming agent to increase the hydrocarbons yield and mitigate CO_2.

2.2. Economic assessment

A comprehensive economic feasibility of a large-scale hybrid biorefinery along with *Jatropha curcas* cultivation in Qatar was evaluated from "well to wheel". The delineated *Jatropha*-Greenbelt (GB) presented earlier as part of this study was considered with 227 km length and 2 km width [25]. For management and cost estimation purposes, the greenbelt was structured into 56 zones (zone area: 2x4 km), while each zone comprised 8 sections (section area: 1x1 km) and each section consisted of 25 *Jatropha* fields (field area: 4 ha) as illustrated in Fig. 2. Each zone was provided with one fruits' storage, while each section contained a diesel-generator, key water storage tank and a pumping station, with a direct TSE supply from the source. In addition, each field was equipped with an independent water dripping system. Key data for *Jatropha* cultivation economics were adapted from previous experiences in Taiwan [66] and India [67], while considering local prices and land

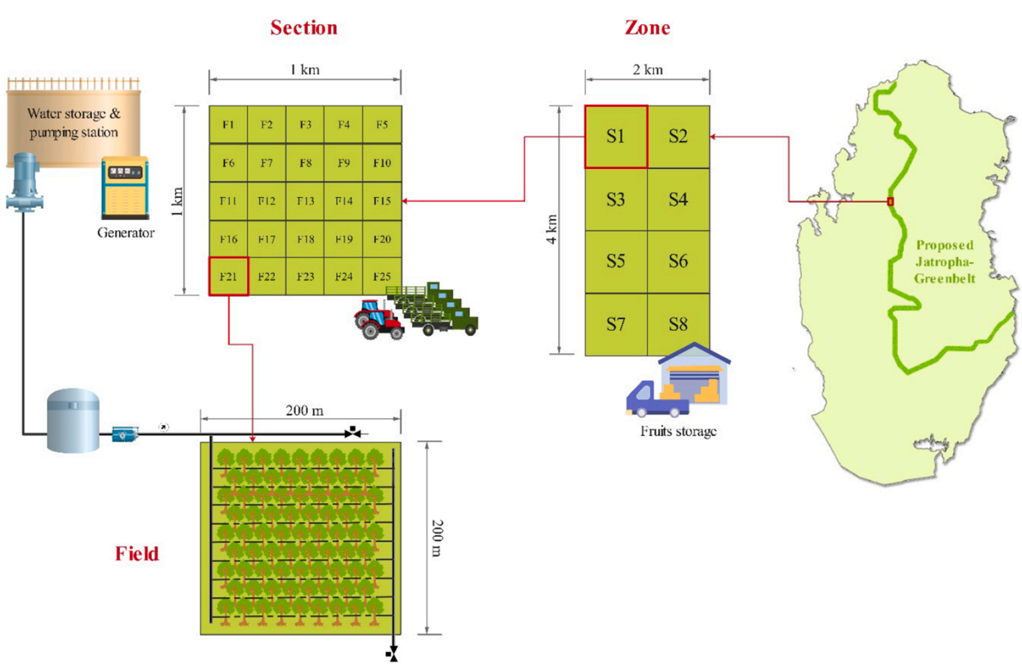

Fig. 2. Managerial division of the proposed *Jatropha*-greenbelt and key cultivation requirement.

Table 2
Key capital expenses of cultivation project.

Stage	Item	No of unites	Price ($/unit)	Ref.
Plantation & Setup	Bulldozer (rental)	2 per section	9,000	[66]
	Leveling machine (rental)	1 per section	4,486	[66]
	Excavator (rental)	1 per section	3,240	[66]
	Diesel fuel (L)	2,550 L per section	0.446	[70]
Growing	Generator (160 kW)	1 per section	26,388	[71]
	Water storage tanks (50 m^3)	1 per section	3,550	[72]
	10hp pumps	1 per section	2,518	[73]
	TSE connections	1 per section	4,110	[2]
	Water dripping system	1 per field	1,360	[74]
	Water distribution tanks	1 per field	92	[75]
	Irrigation pumps	1 per field	142	[76]
	Seedlings	2,222 per field	0.3	[66]
Maintenance & Harvest	Tractor (140 hp)	2 per section	49,850	[66]
	Transportation vehicle (1 t)	4 per section	6,979	[66]
	Harvest baskets	200 per section	6.65	[66]
	Storage containers (20 t)	1 per zone	2,000	[77]

status. As such, 25 % contingencies were considered for plantation and land setup stage due to the harsh structure of Qatar's lands. A summary of cultivation capital expenses is presented in Table 2.

The operational expenses for the cultivation project were mainly associated to fertilisation, irrigation, machineries, maintenance and labour costs. The fertilisers requirement for optimal growth and yield of *Jatropha* was adapted from Suriharn et al. [68], while the energy requirements for machineries were adapted from Neto et al. [69] and Tongpun et al. [66]. Besides, equipment maintenance was considered to be 2 % of the equipment cost on an annual basis.

In addition, the preliminary irrigation requirement for *Jatropha* in the State of Qatar was calculated based on Equation 30 and 31 [78], considering the average reference evapotranspiration in Qatar that was earlier evaluated using the Penman method by Bazaraa [79] and the *Jatropha* crop factors reported by Garg et al. [80] and Lena et al. [81] for the different growing stages. In this project, treated sewage effluent (TSE) was considered to be purchased for irrigation [82]. The amount of diesel required to pump water for irrigation purpose was estimated with an average energy requirement of 0.2 kwh/m^3 and an average pump efficiency of 75 % [83].

$$\mathrm{ET}_{(Jatropha)} = \mathrm{ET}_{(\mathrm{Qatar})} \times \mathrm{K_c} \tag{30}$$

Where, $\mathrm{ET}_{(Jatropha)}$: Evapotranspiration rate of *Jatropha* (mm/day).
$\mathrm{ET}_{o(\mathrm{Qatar})}$: Reference evapotranspiration over the State of Qatar.
$\mathrm{K_c}$: Crop factor of *Jatropha*

$$\mathrm{IWR} = \mathrm{ET}_{(Jatropha)} - \mathrm{R} \tag{31}$$

Where, R: Effective rainfall (mm/day).

The irrigation water requirement (IWR) for *Jatropha* in Qatar was found to be 971, 1295 and 1457 mm/year for the first, second and third year, respectively, as illustrated in Fig. 3. The highest water requirement was witnessed in July with 274 mm/month for mature *Jatropha* trees, while the lowest water requirement was found to be in February with as little as 11 mm/month.

Nevertheless, the labour requirements and costs are evaluated based on a previous report [66] and local survey of wages and salaries [84], as listed in Table A4.

Moreover, the biorefinery economic assessment was established with the aid of Aspen Process Economic Analyser (APEA V.10), considering the set of parameters presented in Table 3. The optimal site for biorefinery establishment was defined in a previous published part of this study at (25°08′38″N, 51°21′03″E) [23]. For capital expenses (CAPEX) evaluation, the key equipment costs were derived from high-level technical reports to establish a more reasonable economic study, as illustrated in Table 4. All equipment prices were scaled-up to the intended capacity and inflated to the base year of analysis (2019) using the Chemical Engineering Plant Cost Index (CEPCI) [85], as formulated in Equation (32) and Equation (33), respectively.

$$Cost_{design} = Cost_{base} * \left(\frac{Capacity_{design}}{Capacity_{base}}\right)^{scalingfactor} \tag{32}$$

$$Cost_{design,\$_{2019}} = Cost_{design,\$_i} \bullet \left(\frac{CEPCI_{2019}}{CEPCI_i}\right) \tag{33}$$

The total CAPEX was estimated based on Equation (34), where the key components of CAPEX were priced in correlation to the inflated purchased equipment costs [99].

$$Capitalexpenses(capex) = Purchasedequipments + Equipmentsetting + Instrumentation + Piping + Buildings + Electrical + Land + Sitedevelopment + Engineering\&Supervision + Contractfees + Construction + Contingencies \tag{34}$$

In addition, the operating expenses (OPEX) is the summation of regular operating costs including raw materials, labour, operating charges, utilities, maintenance and insurance as presented in Equation (35) [99]:

$$Operating\ \ expenses(OPEX) = Feedstock + Raw\ \ materials + Utilities + Labour + Operating\ \ charges + Maintenance + Overhead + Insurance \tag{35}$$

Raw materials prices were quoted as per their average market values, while biomass transportation costs from the supplying source to biorefinery were estimated in ArcGIS considering the biomass distribution in Qatar as presented in Fig. 4 [23]. Whereas labour requirements and charges are validated against a technical report on a biorefinery setup [44] and local salaries [84], as listed in Table A5. Besides, the remaining OPEX components were evaluated using Equations (36–39) [14].

Moreover, the minimum selling prices (MSP) of the different products (i.e., JBF, gasoline and diesel) were evaluated based on the levelised cost of energy concept, considering the products' yield, the plant lifespan, the discount rate and the project CAPEX and OPEX as presented in

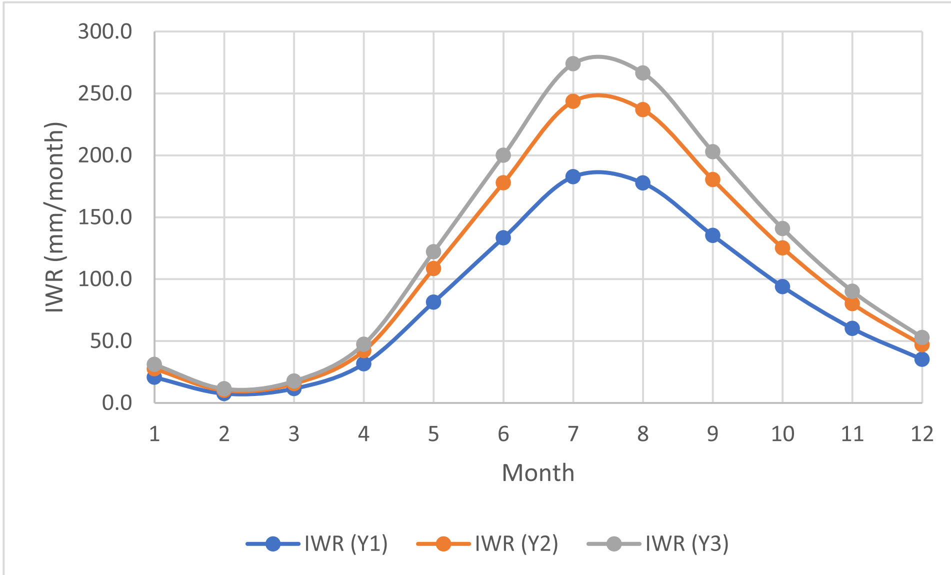

Fig. 3. *Jatropha* irrigation water requirement in Qatar through different growing stages.

Equation (40) [100]. Furthermore, to evaluate the overall feasibility of the project, the return on investment (ROI), net present value (NPV) and the payback period were estimated using Equations (41), (42) and (43), respectively.

$$Operating\ \ charges = 25\%\ \ of\ \ labor\ \ charges \tag{36}$$

$$Maintenance\ \ charges = 2\%\ \ of\ \ purchased\ \ equipment \tag{37}$$

$$Plantoverhead = 50\%oflabor\ \ charges \tag{38}$$

$$Tax\&Insurance = 1.5\%\ \ of\ \ total\ \ installed\ \ costs \tag{39}$$

$$levelized\ \ cost\ \ of\ \ fuel\ \left(\frac{\$}{kg}\right) = \frac{CAPEX + \sum_{1}^{lifespan}\left(OPEX(1+DiscountRate)^{-y}\right)}{\sum_{y=1}^{lifespan}\left(producyield(1+DiscountRate)^{-y}\right)} \tag{40}$$

$$Return\ \ on\ \ investment(ROI)(\%/y) = \frac{Netcashflow}{Initialinvestment} \tag{41}$$

$$NetP\ resent\ Value\ \ (NVP)(\$) = \sum_{y=1}^{lifespan}\frac{Net\ \ cash\ \ flow_y}{(1+Discount\ \ Rate)^y} - Initial\ \ investment \tag{42}$$

$$Payback\ \ period\ \ (years) = \frac{Initial\ \ investment}{Net\ \ cash\ \ flow} \tag{43}$$

2.3. Lifecycle assessment

A comprehensive lifecycle assessment (LCA) of jet biofuel production in the hybrid biorefinery in Qatar was conducted from cradle to grave. Carbon, water, energy and land footprints were selected as the impact categories of the LCA, and were quantified in terms of gCO_2-e, m^3 of water, MJ of energy and cm^2 of land per MJ (JBF), respectively. The carbon footprint was evaluated considering the 5th assessment report on climate change, which is issued and revised by the Intergovernmental Panel on Climate Change (IPCC) [101]. The scope of analysis comprised the *Jatropha* cultivation, biomass transportation, refinery construction, processing and fuel end-use. The different environmental footprints were allocated by energy over the different products and by-products according to their accumulative energy content.

At the cultivation stage, energy and carbon footprints were evaluated based on the diesel consumed in cultivation activities, considering a heating value of 45 MJ/kg and an emission factor of 3.93 $kgCO_2$-e/kg (diesel) [102]. While the amounts of emissions associated to fertilisers were adapted from Lokesh et al. [103]. Furthermore, water and land footprints were completely accounted for at the cultivation stage based on the allocated land for *Jatropha* cultivation, as well as the irrigation water requirement (IWR) estimated earlier. In addition, the carbon dioxide absorbed by *Jatropha* plants through photosynthesis process was assessed to be 2.5 kg CO_2/kg of fruits produced [104].

For the biorefinery setup stage, the construction area required for the plant was estimated based on the refinery siting workbook as a function of plant's capacity [105]. Whereas the required energy, water and associated emissions (per m^2) were adapted from literature [106,107]. While for the biomass transportation stage, the energy consumed and emissions released throughout this stage were adapted from literature as functions of distance travelled and weight transported [108], considering the accumulative distance of all feed transportation estimated in the previous section using ArcGIS.

At the production stage, key values of environmental footprints were obtained through Aspen Plus simulation, while the embodied environmental footprint of raw materials (i.e., hydrogen, methanol) were adapted from literature [109–111], however, it was assumed to be negligible for catalysts. Moreover, the greenhouse gas (GHG) emissions associated to the end-use (combustion) of different fuel products were estimated through process simulation using Aspen Plus [112].

Table 3
Key biorefinery economic parameters and assumptions.

Assumption	Value
Currency	United States Dollar (US $)
Biorefinery location	Qatar (coordinates defined in ArcGIS).
Reference year	2019 (pre-COVID19)
Refinery lifetime	30 years
Input plant capacity	*Jatropha* fruits: 454,000 tonne/year MSW: 530,005 tonne/year Manures: 689,164 tonne/year
Operating hours	8000 hr/year
Engineering, procurement and construction (EPC) phase duration	52 weeks
Contingencies	10 % [62]
Hydrogen gas price	0.7 ($/kg) [86]
Methanol price	0.22 ($/kg) [87]
Hydrotreating catalysts price	34.2 ($/kg) [88]
Hydrocracking catalysts price	117 ($/kg) [61]
Reforming catalyst price	34.2 ($/kg) [88]
Isomerising catalyst price	398 ($/kg) [89]
FT catalyst price	28 ($/kg) [90]
CO_2 gas price	0.15 ($/kg) [91]
TSE price	0.068 $/m^3 [82]
Average jet fuel price (2019)	0.55 ($/kg) [14]
Average diesel price (2019)	1.2 ($/kg) [92]
Average gasoline price (2019)	1.13 ($/kg) [92]

excellent efficiency of the system in jet fuel-mode operation.

The generated jet biofuel can substitute 15.3 % of Qatar's conventional Jet-A, while it can power around one third of its fleet considering a maximum allowable jet biofuel blend of 50 %. Moreover, the generated bio-gasoline and green diesel can substitute 4 % and 5 % of conventional transportation fuels for the year 2016, respectively, as illustrated in Fig. 6. The year 2016 is selected to account for typical Qatar's fuel consumption in pre-Gulf political crisis (2017) and COVID-19 period. Whereby, the aforementioned events have impacted the pattern of fuel consumption, especially for air travel.

Furthermore, out of 1,341,321 tonnes of carbon dioxide produced in the system (operation and power generation), 98.6 % was captured by the carbon capture system. In addition, 41 % of the collected CO_2 was utilised in the system for the dry reforming of methane, while 59 % were stored and sold, as presented in Fig. 7a.

The on-site power station generated around 745 GW annually, whereby, 88.6 % was utilised to power the biorefinery, while 11.4 % was exported to the grid as illustrated in Fig. 7b. The heat integration in the system reduced the refinery's energy requirement, whereby, 538,872 GJ was recovered, which saved over $ 2,500,000 a year.

Nevertheless, the on-site wastewater treatment unit managed to collect the aqueous phase from different sub-units and treated it to a COD level of 193.54 mg/l, which is permissible to be used for industry and agriculture [116]. Only 56 % of treated wastewater was sufficient to fulfil the system water needs including reactions and cooling requirements, while the excess treated effluent was exported to the *Jatropha* field to substitute an equivalent quantity of the purchased TSE, as presented in Fig. 7c.

Table 4
Costs of key biorefinery equipment.

Equipment	Base price (M$)	Base capacity		Design capacity	Scaling factor	Base Year	Ref.
Entrained flow Gasifier	43.25	2,000	t/d	2,081	0.60	2007	[44]
Fischer-Tropsch slurry reactor	326.87	50,000	FT bbl/d	3,453	0.88	2006	[93]
Plug flow reformer	10.71	33,360	kmol/d	64,656	0.60	2003	[94]
Hydrotreater (1)	2.22	74	t/d	768	0.70	2011	[95]
Hydrotreater (2)	2.22	74	t/d	225.12	0.70	2011	[95]
Hydrocracker	9.30	100	t/d	692.4	0.55	2007	[96]
Isomerisation unit	0.95	13	t/d	692.4	0.62	2007	[96]
Combustion turbine generator	69.57	80	MW	93	0.70	2006	[93]
Absorption system (1)	0.43	70	t/d	317	0.75	2007	[44]
Absorption system (2)	0.43	70	t/d	3424	0.75	2007	[44]
HTL reactors	80.00	2,000	t/d	1886.83	1	2007	[97]
Rotary dryer	0.68	2,000	t/d	2,406	0.7	2010	[98]
Grinding hammer mill	0.30	2,000	t/d	2,406	0.7	2010	[98]

Finally, the land, energy, water and emissions savings achieved in the process were deducted from the overall environmental footprints. These savings include the reduction in landfill area and the associated emissions through the utilisation of MSW [113,114], as well as emissions reduction due to the prevention of natural decomposition of livestock manures [115]. In addition to the energy and water substitution through the excess utilities generated within the system.

3. Results and discussion

Along with the design of a hybrid biorefinery, its optimal location has been identified in Qatar using ArcGIS approach, while its candidate feedstocks have been selected through the developed predictive model. The following subsections detail the obtained results.

3.1. Process' outputs

Due to the intensive integration of streams within the hybrid biorefinery, liquid fuels yields were maximised, where neither char nor gas products were produced, but rather utilised within the system. As illustrated in Fig. 5, the system generated around 466 million litres of liquid fuels per year, with jet fuel occupying 72 %, followed by gasoline and diesel at 18 % and 10 %, respectively. Around 24 % of the biomass feed (dry and ash free) has been converted into jet fuel, which reflects an

3.2. Jet biofuel characteristics

The generated JBF in the proposed hybrid biorefinery was characterised to ensure meeting international criteria (ASTM D7566). As revealed in Table 5, all chemical and physical criteria of generated JBF perfectly complied with Jet-A standards. As compared to the stand-alone *Jatropha* biorefinery which was presented in author's earlier study [14], the inclusion of the HTL stream into the refinery provided the missing aromatics components to the fuel, which is important to prevent tank leakage (with maximum JBF aromatics of 25 vol%) [6]. As a result, the density of fuel has also been enhanced to fall within the accepted range. The fuel's flash point was slightly high, but still complies with the standards. Fuels with higher flash points are safer to store and handle, especially in hot regions like Qatar.

3.3. Economic performance

A summary of the project's economics is presented in Table 6. The total investment cost was at $ 1,332,038,426, which was estimated to be

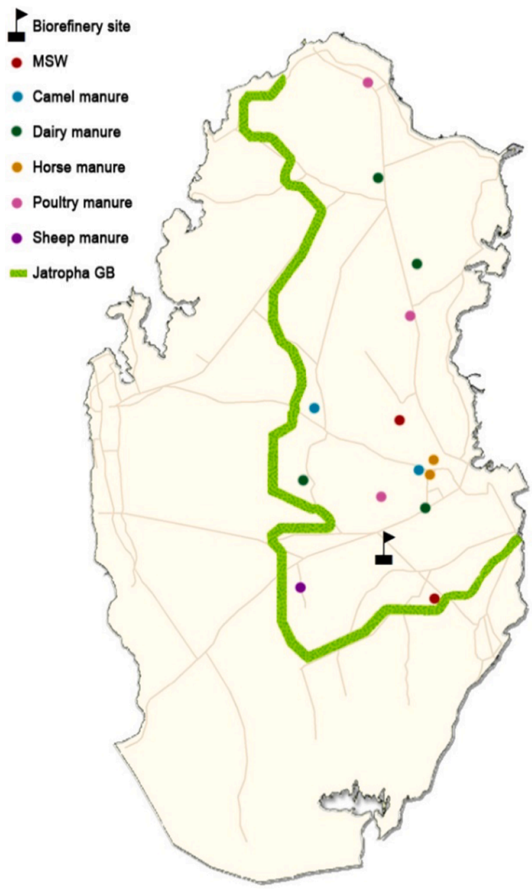

Fig. 4. Biorefinery site and selected biomass' geospatial distribution in Qatar.

paid back in around 11 years, with 10.8 % return on investment (ROI). The sub-CAPEX required for the biorefinery establishment was higher than that of the *Jatropha* field, in contrast to OPEX, which was higher for the cultivation part of the project due to the manpower requirement. The total OPEX was estimated at $ 215,696,583 a year.

A high start-up cost of $ 205,055,959 a year was assigned to cover all costs before the refinery starts operating. Whereby, the first two years of plantation, minimal *Jatropha* fruits are obtained, while the full yield is obtained starting from year 4. However, it was assumed that the accumulative quantity of fruits during year 1–3 together is equivalent to year 4 yield and is utilised in year 3. The manpower requirement was 8,252 employees, most of whom were assigned to *Jatropha* field maintenance, while 184 employees were hired to manage and operate the biorefinery.

Capital Expenses (CAPEX):

At the cultivation level, land costs were excluded, assuming the project is government-backed, and the lands used are all public. As such, the highest sub-CAPEX component was associated to key machineries including tractors and transportation vehicles (>50 %) as presented in Fig. 8. While the equipment items related to irrigation accounted for around 30 % of sub-CAPEX, which included tanks, pumps, generators, and water dripping systems. While the land preparation and set-up accounted for around 12 %.

The breakdown of sub-CAPEX associated to biorefinery establishment is illustrated in Fig. 9. Whereby, the purchased equipment occupies around 40 %, followed by construction expenses, service facilities and engineering works, with around 8 % each. Nevertheless, the breakdown of purchased equipment costs is presented in Fig. 10. The combustion-turbine generator occupied quarter of total equipment costs, followed by HTL reactors (22 %), gasification unit (13 %), FT reactor (9 %), and hydrocracking reactor (8 %). The high cost of power generation unit is associated to its high capacity and efficiency, while the high cost of the HTL reactors is due to the use of multiple separate reactors, as large-scale reactors are still in the research and development phase due to complexity of handling large slurry streams at extremely high pressure.

Operational Expenses (OPEX):

The dominant component of sub-OPEX at cultivation stage was the labour costs, with around 56 %. Whereby a substantial number of manpower was required to handle the large *Jatropha* field (454 km^2). Irrigation associated water and energy requirements occupied 17 % and 6 % respectively, while fertilisers accounted for 16 % of sub-OPEX, as illustrated in Fig. 11.

Furthermore, the costs associated to raw materials provision and transportation (including feedstocks) occupied around 62 % of the biorefinery's sub-OPEX. The highest raw material cost was associated to hydrogen use, which could be generated on-site in future biorefinery designs to reduce costs and environmental impact. While insurance and labour costs accounted for 13 % and 9 % of sub-OPEX, respectively, as

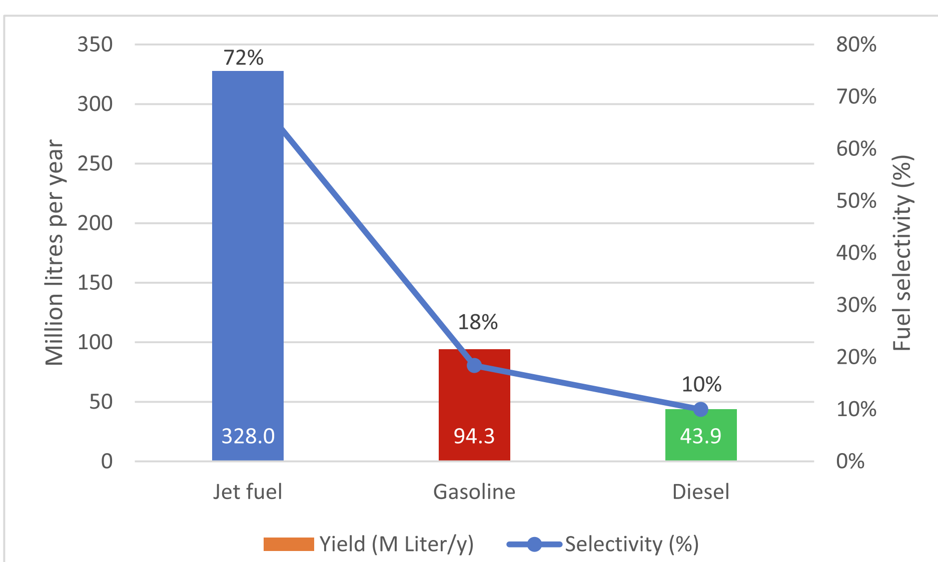

Fig. 5. Biorefinery fuel yields (M litres/y) and selectivity (%).

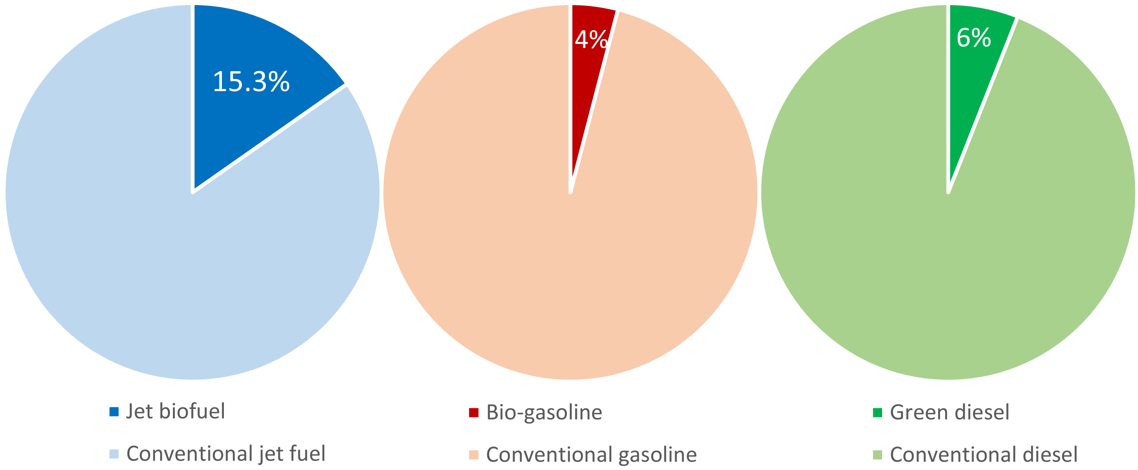

Fig. 6. Generated green fuels substitution of fossil fuels in Qatar for the year 2016.

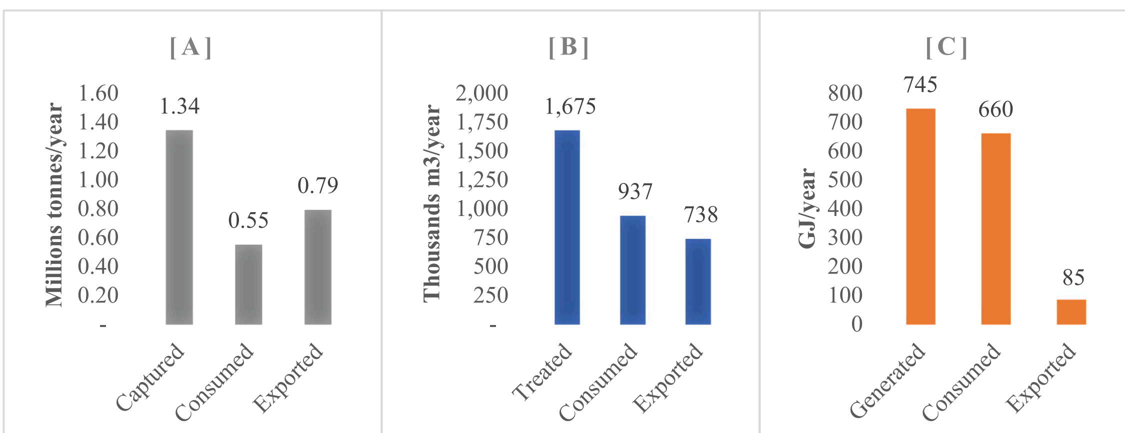

Fig. 7. Production, consumption and export of (a) CO_2, (b) water, (c) power.

presented in Fig. 12.

NPVs and MSPs:

The net present value (NPV) of the investment which accounts for the time value of the cash flow was evaluated using different discount rates as presented in Fig. 13. At an average discount rate of 8 %, the NPV was found at $ 289,014,873. The NPV of the investment was positive at discount rate of 10 %, which is commonly used as a reference (named: PV-10) for the oil industries [118]. However, the discount rate of 10.22 % represented a breakeven point, beyond which the NPV of the project became negative. As such, the project is considered feasible as long as the estimated discount rate does not exceed 10.22 %.

Nevertheless, the minimum selling prices (MSPs) of different fuels

Table 5
Characteristics of generated JBF as compared to international standards.

Parameter	Unit	Conventional Jet-A [117] (ASTM D7566)	JBF of the Hybrid Biorefinery (This study)
Net heating value	MJ/kg	> 42.8	43.6
Density @ 15 °C	kg/m^3	775–840	791.4
Kinematic viscosity	mm^2/s	< 8	3.95
Average boiling point	°C	170–300	236
Flash point	°C	> 38	73
Freeze point	°C	< −40	−53
Olefins' content	wt.%	< 1 %	0.87 %
Sulfur content	wt.%	< 0.003	1×10^{-9}
Aromatics	vol.%	8–25	9.6

Table 6
A summary of the project's economics.

Parameter	Value	Unit
Total CAPEX	1,332,038,426	$
Sub-CAPEX (*Jatropha* field)	318,136,361	$
Sub-CAPEX (Biorefinery)	1,013,902,065	$
Total OPEX	215,696,583	$/y
Sub-OPEX (*Jatropha* field)	124,683,849	$/y
Sub-OPEX (Biorefinery)	91,012,733	$/y
Start-up cost (2 years)	205,055,959	$
Total number of employees	8,252	
Number of employees (*Jatropha* field)	8,068	
Number of employees (Biorefinery)	184	
Total labour cost	77,379,600	$/y
JBF minimum selling price (DR: 8 %)	0.430	$/kg
Gasoline minimum selling price (DR: 8 %)	0.663	$/kg
Diesel minimum selling price (DR: 8 %)	0.337	$/kg
Annual sales	359,690,586	$/y
Annual profit	143,994,004	$/y
Return on investment	10.81	%/y
Net present value (DR: 8 %)	289,014,873	$
Payback period	11.25	Years

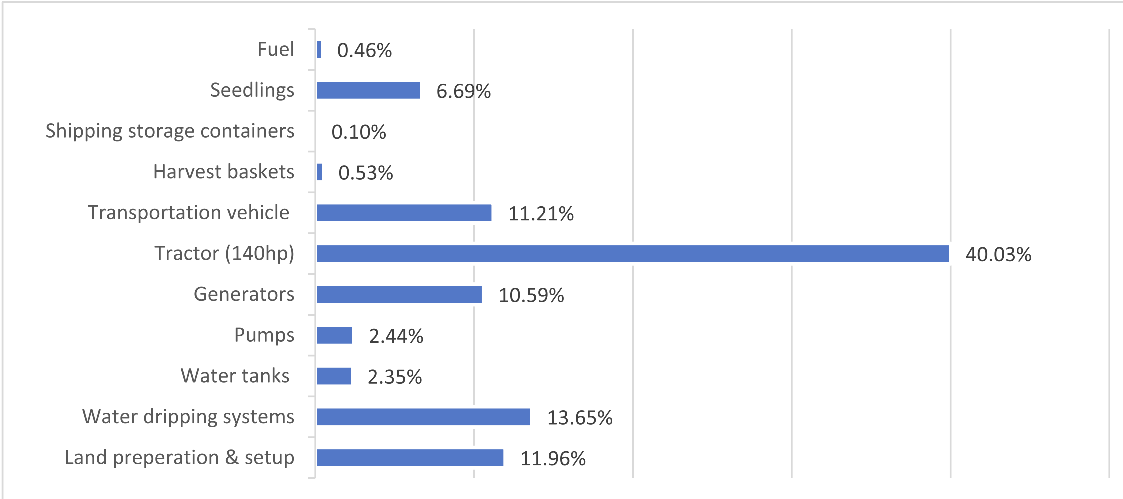

Fig. 8. Breakdown of sub-CAPEX for the cultivation part of the project.

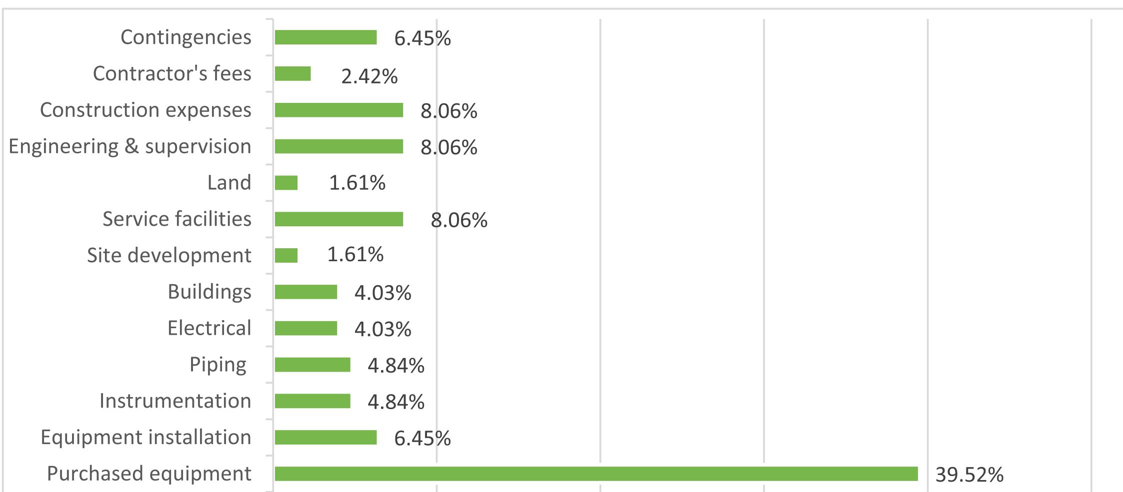

Fig. 9. Breakdown of sub-CAPEX for the biorefinery establishment part of the project.

were evaluated using different discount rates, as illustrated in Fig. 14. At an average discount rate of 8 %, the produced jet biofuel can be sold at a competitive minimum price of 0.43 $/kg, which is 22 % lower than conventional Jet-A market price. While bio-gasoline can be sold at 0.66 $/kg, which is 41 % lower than conventional gasoline market price, and it is close to the local subsidised retail price of 0.62 $/kg [70]. Likewise, green diesel can be sold at as low as 0.33 $/kg. All three biofuels can still be sold below the market price of their corresponding conventional fuels while increasing the discount rate up to 10.48 %, at which the biofuels' minimum selling prices are equal to the market prices of conventional fossil fuels. It can be concluded that the investment is feasible and the minimum selling prices of biofuels are competitive as long as the forecasted discount rate is at a maximum of 10.22 %.

3.4. Environmental performance

A comprehensive lifecycle environmental assessment for JBF production was conducted from cradle to grave (well to wheel). A summary of the findings for energy, carbon, water and land footprints is presented through Tables 7, 8, 9 and 10, respectively.

As for energy footprint, cultivation contributed to a higher energy consumption than production stage, with fertilisers being the dominant energy-consuming step at 31 % out of the net energy consumption and 38 % out of the cultivation energy requirement, while irrigation-related energy consumption was estimated at 29 % out of the net energy footprint. Power was completely generated on-site, and heat is circulated and utilised within the system, therefore, the embodied energy of raw materials was the largest energy-consuming component at production stage with a share of 13 % out of the net energy footprint. The net energy footprint of jet biofuel produced in this study was estimated at 0.13 MJ/MJ_{JBF}, indicating a high energy efficiency of the hybrid system and an effective management and utilisation of heat and power products.

Whereas for the carbon footprint, the fuel's end-use was responsible for the biggest portion of emissions throughout its lifecycle, with around 70 %. Exclusive of end-use stage, the key component of the carbon footprint was the raw materials at ~ 65 %, followed by the cultivation stage with 30 %. Obviously, the employment of carbon capture system has greatly contributed to emissions reduction at the processing level. Meanwhile, the utilisation of multiple biomass enhanced the fuel's lifecycle through different carbon saving routes. Whereby, the use of manures prevented the release of emissions (i.e., methane) from its natural decomposition.

Besides, the involvement of municipal solid wastes contributed to landfill diversion, which reduces multiple environmental harms. Nevertheless, energy crops such as *Jatropha* is considered the most effective biomass for CO_2 abatement, whereby, the crop can uptake

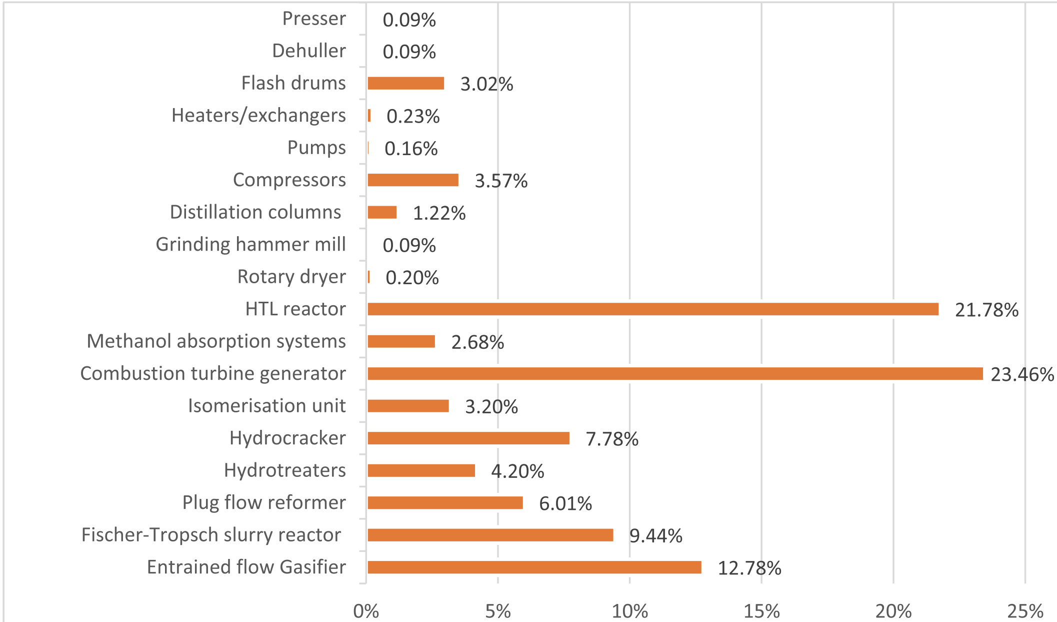

Fig. 10. Breakdown of biorefinery's purchased equipment.

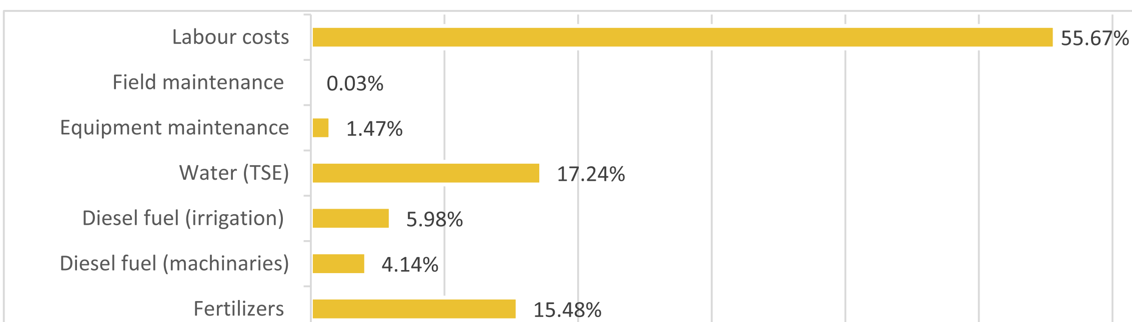

Fig. 11. Breakdown of cultivation sub-OPEX.

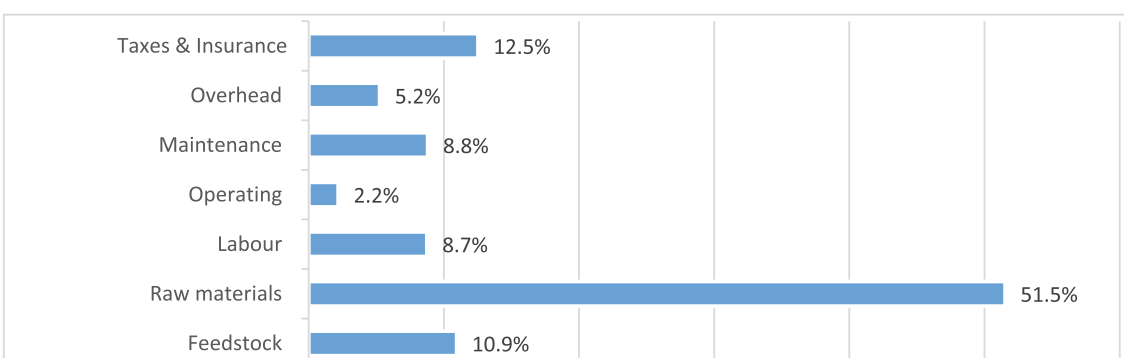

Fig. 12. Breakdown of biorefinery's sub-OPEX.

almost an equivalent amount of CO_2 through photosynthesis process to that released at end-use (carbon neutral). The net carbon footprint of JBF was estimated at 53 gCO_2-e/ MJ (JBF), which indicated a 41 % mitigation in GHG emissions as compared to the Jet-A fuel [112].

As compared to the stand-alone *Jatropha* biorefinery [14], the hybrid system managed to further enhance the fuel's lifecycle, through intensive integration of streams, as well as the involvement of carbon capture techniques.

In addition, the water footprint of jet biofuel production was extremely dominated by the irrigation of *Jatropha* crop, with around 99 % out of the net water consumption. Although treated sewage effluent is utilised instead of fresh water, it has been completely accounted for. Whereas annual rainwater is not considered in the calculations due to irregular and marginal precipitation levels in Qatar. At the production stage, no water is consumed as all aqueous phases are collected, treated and re-used within the system with a significant surcharge. However,

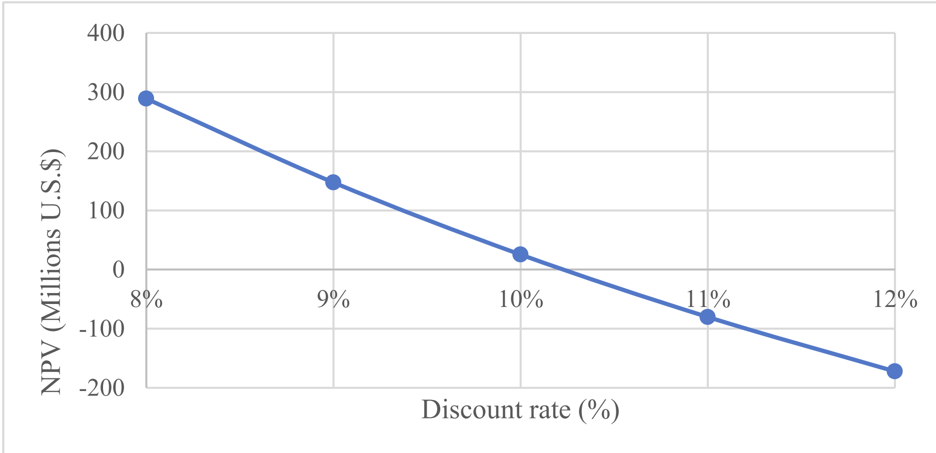

Fig. 13. Net present value of the investment (million $) at different discount rates.

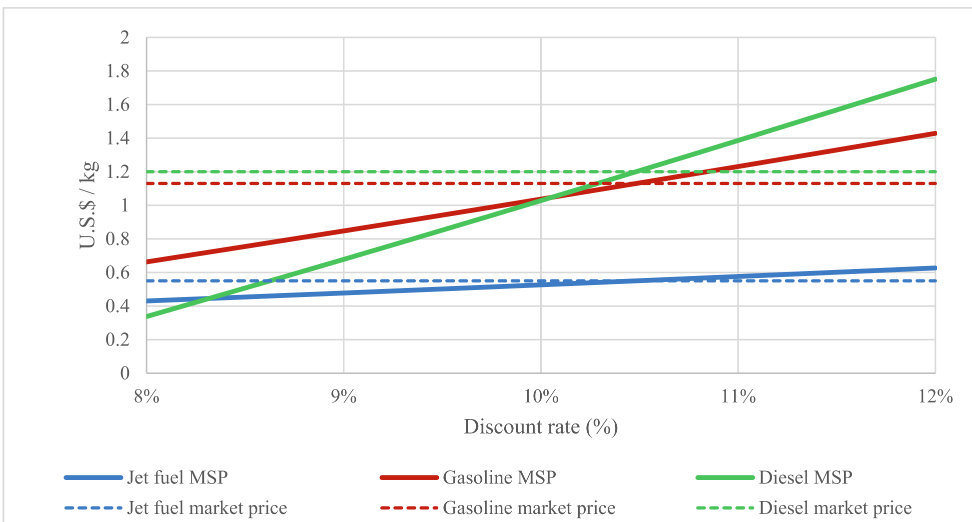

Fig. 14. Minimum selling prices of fuel products as compared to market price (2019).

Table 7
Breakdown of jet biofuel's lifecycle energy footprint.

Stage	Sub-stage	Value (MJ/lifespan)
Cultivation	Land set-up	44.28×10^6
	Fertilisers	$20{,}653 \times 10^6$
	Irrigation	$19{,}305 \times 10^6$
	Machineries	$14{,}170 \times 10^6$
Production	Transportation	$3{,}102 \times 10^6$
	Refinery construction	25.4×10^6
	Raw materials	$8{,}437 \times 10^6$
	Processing (saving)	$-9{,}210 \times 10^6$
Total (MJ/lifespan)		$56{,}526 \times 10^6$
Energy footprint		**0.13 (MJ / MJ jet biofuel)**

Table 8
Breakdown of jet biofuel's lifecycle carbon footprint.

Stage	Sub-stage	Value (tonne CO_2-e/lifespan)
Cultivation	Land set-up	3.82×10^3
	Fertilisers	259.2×10^3
	Irrigation	$1{,}665 \times 10^3$
	Machineries	$1{,}222 \times 10^3$
	Jatropha emissions uptake	-1.44×10^7
Production	Transportation	8.9×10^3
	Refinery construction	16.9×10^3
	Raw materials	6.9×10^3
	Processing emissions	409×10^3
	Manure utilisation (saving)	-614×10^3
	Landfill diversion (saving)	−653
	Electricity substitution	$-1{,}058 \times 10^3$
End-use	Fuel combustion	2.2×10^7
Total (tonne CO_2-e/lifespan)		$16{,}675 \times 10^3$
Carbon footprint		**53 (gCO_2-e/ MJ jet biofuel)**

the embodied water from the raw materials production (mainly H_2) was accounted for, whereby, hydrogen is often produced through steam reforming of natural gas (SMR), with around 15 L of water per each 1 kg of hydrogen produced. The net water footprint was evaluated at 0.023 m^3/ MJ (JBF).

Finally, the land footprint was estimated at 0.001 m^2 per MJ (JBF) throughout the lifespan of the project. Land was dominantly used for the cultivation of *Jatropha*. However, the selected lands are classified as non-arable [25], as such, the use of these lands to grow energy crops was not at the expense of food cultivation. In contrast, growing *Jatropha* in arid area may enhance its soil through aeration and the supply of organic matter by dropped leaves and fruit residues [26]. Nevertheless, landfill diversion was achieved through the utilisation of MSW, which contributes to saving around 197,000 m^2, assuming an average MSW specific weight of 6 tonne/m^3 and a landfill depth of 15 m.

Table 9
Breakdown of jet biofuel's lifecycle water footprint.

Stage	Sub-stage	Value (m^3/lifespan)
Cultivation	Growing	$10{,}074 \times 10^6$
Production	Refinery construction	0.76×10^6
	Raw materials	21.4×10^6
	Processing (saving)	-22.12×10^6
Total (m^3/lifespan)		$10{,}053 \times 10^6$
Water footprint		**0.023 (m^3/ MJ jet biofuel)**

Table 10
Breakdown of jet biofuel's lifecycle land footprint.

Stage	Sub-stage	Value (m^2/lifespan)
Cultivation	Cultivated land	454×10^6
Production	Refinery site	28.2×10^3
	Landfill diversion (saving)	-197×10^3
Total (m^2/lifespan)		453.8×10^6
Land footprint		**10.4 (cm^2/ MJ jet biofuel)**

Table 11
Evaluation of the produced JBF against CORSIA and RSB standards.

CORSIA standard [119]	RSB standard [120]	JBF features (this study)
Eligible fuel should generate at least 10 % lower carbon emissions on a life cycle basis.	Eligible fuel should generate 50–60 % lower carbon emissions on a life cycle basis.	JBF achieved 41 % lower carbon emissions on a life cycle basis.
Eligible fuel should not be made from biomass obtained from land with high carbon stock.		Only barren lands are considered for the growing of *Jatropha* energy crops.
	Eligible feedstock: (primary biomass, wastes, residues, by products).	Feedstock used are within the eligible RSB classes: Primary biomass: Jatropha. Residues: Manure. Waste: MSW.

Nevertheless, the produced JBF was assessed against the CORSIA and the roundtable sustainable biomaterials (RSB) standards as illustrated in Table 11. The emissions reduction requirement by CORSIA (>10 %) was strictly met by the proposed JBF (41 %), however, it was still slightly below the RSB high standard of 50–60 % emissions reduction, which could be enhanced by the involvement of new low-emission feedstocks such as waste cooking oil. Whereas the proposed JBF has met all other CORSIA and RSB criteria including approved feedstock, low-carbon stock lands and adequate LCA calculation methods.

4. Conclusion

This study has proposed a novel design of a hybrid biorefinery to produce jet biofuel using multiple biomass resources available in the State of Qatar. The model was developed in Aspen Plus, which comprised key advanced and mostly well-established processes including hydroprocessing, Fischer-Tropsch, reforming, gasification and hydrothermal liquefaction. Intensive integration of streams was performed to maximise JBF production and minimise solid and gaseous by-products, while the system was equipped with a carbon capture, power generation and wastewater treatment units to enhance its environmental performance. The system generated 328, 94 and 44 million litres of JBF, gasoline and diesel, respectively, which can substitute 15.3 %, 4 % and 6 % of the corresponding conventional fuels in Qatar. Produced JBF was characterised and found to comply with all international standards. It is believed that the fuel is suitable to be directly utilised as a drop-in fuel without the need for any additives, blending with other fuel, or modification to existing jet engines.

The project capital investment cost was estimated at $ 1,332,038,426, with an ROI of ~ 11 and ~ 11 years of payback period. The produced JBF achieved an MSP of 0.43 $/kg, which is 22 % lower than the market price of conventional jet fuel (2019). In addition, the environmental performance of JBF was evaluated from well to wheel. Whereby, an energy, water, land and carbon footprints of 0.13 MJ, 0.023 m^3, 10.4 cm^2 and 53 gCO_2-e per MJ (JBF) were achieved, respectively. Produced JBF is found to contribute to 41 % mitigation in GHG emissions as compared to the conventional Jet-A fuel.

CRediT authorship contribution statement

Mohammad Alherbawi: Conceptualization, Methodology, Software, Validation, Formal analysis, Investigation, Resources, Data curation, Writing – original draft, Visualization. **Gordon McKay:** Conceptualization, Methodology, Project administration, Supervision, Conceptualization, Methodology, Writing – review & editing. **Tareq Al-Ansari:** Project administration, Supervision, Conceptualization, Methodology, Writing – review & editing.

Declaration of Competing Interest

The authors declare that they have no known competing financial interests or personal relationships that could have appeared to influence the work reported in this paper.

Data availability

No data was used for the research described in the article.

Acknowledgements

The authors would like to acknowledge Hamad Bin Khalifa University (HBKU), a member of the Qatar Foundation (QF) for supporting this research. Open Access funding provided by the Qatar National Library.

Appendix A. Supplementary material

Supplementary data to this article can be found online at https://doi.org/10.1016/j.enconman.2022.116569.

References

[1] WBA. Global Bioenergy Statistics 2019; 2019.
[2] Alherbawi M, Parthasarathy P, Al-Ansari T, Mackey HR, McKay G. Potential of drop-in biofuel production from camel manure by hydrothermal liquefaction and biocrude upgrading: A Qatar case study. Energy 2021::121027. https://doi.org/10.1016/j.energy.2021.121027.
[3] ICAO. Sustainable Aviation Fuels Guide. 2017.
[4] Gutiérrez-Antonio C, Romero-Izquierdo AG, Gómez-Castro FI, Hernández S, Briones-Ramírez A. Simultaneous energy integration and intensification of the hydrotreating process to produce biojet fuel from Jatropha curcas. Chem Eng Process Process Intensif 2016;110:134–45. https://doi.org/10.1016/j.cep.2016.10.007.
[5] Li M, Fu J, Xing S, Yang L, Zhang X, Lv P, et al. A novel catalyst with variable active sites for the direct hydrogenation of waste oils into jet fuel. Appl Catal B Environ 2020;260:118114. https://doi.org/10.1016/j.apcatb.2019.118114.
[6] Alherbawi M, McKay G, Mackey HR, Al-Ansari T. Jatropha curcas for jet biofuel production: Current status and future prospects. Renew Sustain Energy Rev 2021;135:110396. https://doi.org/10.1016/j.rser.2020.110396.
[7] Alherbawi M, Parthasarathy P, Al-Ansari T, Mckay G. Potential of Biocrude Production from Camel Manure via Hydrothermal Liquefaction: A Qatar Case Study. 12th Int. Exergy, Energy Environ. Symp. (IEEES-12), Doha, Qatar, vol. 12, 2020, p. 357–60.
[8] Sadhukhan J, Sen S. A novel mathematical modelling platform for evaluation of a novel biorefinery design with Green hydrogen recovery to produce renewable aviation fuel. Chem Eng Res Des 2021;175:358–79. https://doi.org/10.1016/j.cherd.2021.09.014.

[9] Kumar D, Long SP, Singh V. Biorefinery for combined production of jet fuel and ethanol from lipid-producing sugarcane: a techno-economic evaluation. GCB Bioenergy 2018;10:92–107. https://doi.org/10.1111/gcbb.12478.

[10] Santos CI, Silva CC, Mussatto SI, Osseweijer P, van der Wielen LAM, Posada JA. Integrated 1st and 2nd generation sugarcane bio-refinery for jet fuel production in Brazil: Techno-economic and greenhouse gas emissions assessment. Renew Energy 2018;129:733–47.

[11] Wang W-C. Techno-economic analysis of a bio-refinery process for producing Hydro-processed Renewable Jet fuel from Jatropha. Renew Energy 2016;95:63–73. https://doi.org/10.1016/j.renene.2016.03.107.

[12] Romero-Izquierdo AG, Gómez-Castro FI, Hernández S, Gutiérrez-Antonio C. Computer aided-design of castor bean fruit-based biorefinery scheme to produce sustainable aviation fuel. Chem Eng Res Des 2022;188:746–63.

[13] Tanzil AH, Brandt K, Zhang X, Wolcott M, Silva Lora EE, Stockle C, et al. Evaluation of bio-refinery alternatives to produce sustainable aviation fuels in a sugarcane mill. Fuel 2022;321:123992. https://doi.org/10.1016/j.fuel.2022.123992.

[14] Alherbawi M, McKay G, Mackey HR, Al-Ansari T. A novel integrated pathway for Jet Biofuel production from whole energy crops: A Jatropha curcas case study. Energy Convers Manag 2021;229:113662. https://doi.org/10.1016/j.enconman.2020.113662.

[15] Julio AAV, Batlle EAO, Trindade AB, Nebra SA, Reyes AMM, Palacio JCE. Energy, exergy, exergoeconomic, and environmental assessment of different technologies in the production of bio-jet fuel by palm oil biorefineries. Energy Convers Manag 2021;243:114393.

[16] Romero-Izquierdo AG, Gómez-Castro FI, Gutiérrez-Antonio C, Barajas RC, Hernández S. Development of a biorefinery scheme to produce biofuels from waste cooking oil. Comput. Aided Chem. Eng., vol. 46, Elsevier; 2019, p. 289–94.

[17] Bezergianni S, Dimitriadis A, Kikhtyanin O, Kubička D. Refinery co-processing of renewable feeds. Prog Energy Combust Sci 2018;68:29–64. https://doi.org/10.1016/j.pecs.2018.04.002.

[18] Menon V, Rao M. Trends in bioconversion of lignocellulose: Biofuels, platform chemicals & biorefinery concept. Prog Energy Combust Sci 2012;38:522–50. https://doi.org/10.1016/j.pecs.2012.02.002.

[19] Maity SK. Opportunities, recent trends and challenges of integrated biorefinery: Part I. Renew Sustain Energy Rev 2015;43:1427–45. https://doi.org/10.1016/j.rser.2014.11.092.

[20] Heidenreich S, Foscolo PU. New concepts in biomass gasification. Prog Energy Combust Sci 2015;46:72–95. https://doi.org/10.1016/j.pecs.2014.06.002.

[21] Budzianowski WM, Postawa K. Total Chain Integration of sustainable biorefinery systems. Appl Energy 2016;184:1432–46. https://doi.org/10.1016/j.apenergy.2016.06.050.

[22] Özdenkçi K, De Blasio C, Muddassar HR, Melin K, Oinas P, Koskinen J, et al. A novel biorefinery integration concept for lignocellulosic biomass. Energy Convers Manag 2017;149:974–87. https://doi.org/10.1016/j.enconman.2017.04.034.

[23] Alherbawi M, Mckay G, Mackey HR, Al-Ansari T. Multi-biomass Refinery Siting: a Gis Geospatial Optimization Approach. Chem Eng Trans 2022;92:73–8.

[24] Alherbawi M, AlNouss A, Govindan R, McKay G, Al-Ansari T. A predictive model for multi-criteria selection of optimal thermochemical processing pathways in biorefineries. Comput. Aided Chem. Eng., vol. 49, Elsevier; 2022, p. 949–54.

[25] Alherbawi M, McKay G, Govindan R, Haji M, Al-Ansari T. A novel approach on the delineation of a multipurpose energy-greenbelt to produce biofuel and combat desertification in arid regions. J Environ Manage 2022;323:116223. https://doi.org/10.1016/j.jenvman.2022.116223.

[26] Tomar NS, Ahanger MA, Agarwal RM. Jatropha curcas: An Overview. In: Ahmad P, Wani MR, editors. Physiol. Mech. Adapt. Strateg. Plants Under Chang. Environ. Vol. 2, New York, NY: Springer New York; 2014, p. 361–83. https://doi.org/10.1007/978-1-4614-8600-8_13.

[27] Singh RN, Vyas DK, Srivastava NSL, Narra M. SPRERI experience on holistic approach to utilize all parts of Jatropha curcas fruit for energy. Renew Energy 2008;33:1868–73. https://doi.org/10.1016/j.renene.2007.10.007.

[28] Alherbawi M, AlNouss A, Mckay G, Al-Ansari T. Optimum Utilization of Jatropha Seedcake Considering the Energy, Water and Food Nexus. In: Pierucci S, Manenti F, Bozzano GL, Manca DBT-CACE, editors. 30 Eur. Symp. Comput. Aided Process Eng., vol. 48, Elsevier; 2020, p. 229–34. 10.1016/B978-0-12-823377-1.50039-2.

[29] Ye M, Li C, Francis G, Makkar HPS. Current situation and prospects of Jatropha curcas as a multipurpose tree in China. Agrofor Syst 2009;76:487–97.

[30] Islam AKMA, Yaakob Z, Anuar N. Jatropha: A multipurpose plant with considerable potential for the tropics. Sci Res Essays 2011;6:2597–605.

[31] Salimon J, Ahmed WA. Physicochemical Characteristics of Tropical Jatropha curcas Seed Oil. Sains Malaysiana 2012;41:313–7.

[32] Al-Ansari T, AlNouss A, Al-Thani N, Parthasarathy P, ElKhalifa S, Mckay G, et al. Optimising Multi Biomass Feedstock Utilisation Considering a Multi Technology Approach. In: Pierucci S, Manenti F, Bozzano GL, Manca DBT-CACE, editors. 30 Eur. Symp. Comput. Aided Process Eng., vol. 48, Elsevier; 2020, p. 1633–8. 10.1016/B978-0-12-823377-1.50273-1.

[33] Yuan X, He T, Cao H, Yuan Q. Cattle manure pyrolysis process: Kinetic and thermodynamic analysis with isoconversional methods. Renew Energy 2017;107:489–96. https://doi.org/10.1016/j.renene.2017.02.026.

[34] Chong CT, Mong GR, Ng J-H, Chong WWF, Ani FN, Lam SS, et al. Pyrolysis characteristics and kinetic studies of horse manure using thermogravimetric analysis. Energy Convers Manag 2019;180:1260–7. https://doi.org/10.1016/j.enconman.2018.11.071.

[35] Katsaros G, Pandey DS, Horvat A, Almansa GA, Fryda LE, Leahy JJ, et al. Gasification of poultry litter in a lab-scale bubbling fluidised bed reactor: Impact of process parameters on gasifier performance and special focus on tar evolution. Waste Manag 2019;100:336–45.

[36] Akyürek Z. Synergetic Effects during Co-Pyrolysis of Sheep Manure and Recycled Polyethylene Terephthalate. Polymers (Basel) 2021;13:2363.

[37] Ramírez V, Martí-Herrero J, Romero M, Rivadeneira D. Energy use of Jatropha oil extraction wastes: Pellets from biochar and Jatropha shell blends. J Clean Prod 2019;215:1095–102. https://doi.org/10.1016/j.jclepro.2019.01.132.

[38] Parthasarathy P, Alherbawi M, Pradhan S, Al-Ansari T, Mackey HR, McKay G. Pyrolysis characteristics, kinetic, and thermodynamic analysis of camel dung, date stone, and their blend using thermogravimetric analysis. Biomass Convers Biorefinery 2022:1–18.

[39] Alnouss A, Mckay G, Al-ansari T. Optimum Utilization of Biomass for the Production of Power and Fuels using Gasification. 28th Eur. Symp. Comput. Aided Process Eng., vol. 43, Elsevier Masson SAS; 2018, p. 1481–6. https://doi.org/10.1016/B978-0-444-64235-6.50258-8.

[40] Zhong C, Wei X. A comparative experimental study on the liquefaction of wood. Energy 2004;29:1731–41.

[41] Demirbaş A. Relationships between lignin contents and fixed carbon contents of biomass samples. Energy Convers Manag - ENERG CONV Manag 2003;44:1481–6. https://doi.org/10.1016/S0196-8904(02)00168-1.

[42] Magdeldin M, Kohl T, Järvinen M. Techno-economic Assessment of Integrated Hydrothermal Liquefaction and Combined Heat and Power Production from Lignocellulose Residues. J Sustain Dev Energy, Water Environ Syst 2018;6:89–113.

[43] Lentz Z, Kolar P, Classen J. Valorization of Swine Manure into Hydrochars. Processes 2019;7:560. https://doi.org/10.3390/pr7090560.

[44] National Renewable Energy Laboratory. Process Design and Economics for Conversion of Lignocellulosic Biomass to Ethanol. 2011.

[45] AlNouss A, McKay G, Al-Ansari T. Production of syngas via gasification using optimum blends of biomass. J Clean Prod 2020;242:118499. https://doi.org/10.1016/j.jclepro.2019.118499.

[46] Iqbal S, Davies TE, Morgan DJ, Karim K, Hayward JS, Bartley JK, et al. Fischer Tropsch synthesis using cobalt based carbon catalysts. Catal Today 2016;275:35–9. https://doi.org/10.1016/j.cattod.2015.09.041.

[47] Bermudez JM, Fidalgo B. 15 - Production of bio-syngas and bio-hydrogen via gasification. In: Luque R, Lin CSK, Wilson K, Clark JBT-H of BP (Second E, editors., Woodhead Publishing; 2016, p. 431–94. 10.1016/B978-0-08-100455-5.00015-1.

[48] Fox JM. Fischer-Tropsch reactor selection Catal Letters 1990;7:281–92. https://doi.org/10.1007/BF00764509.

[49] Schulz H. Short history and present trends of Fischer-Tropsch synthesis. Appl Catal A Gen 1999;186:3–12. https://doi.org/10.1016/S0926-860X(99)00160-X.

[50] AlNouss A, McKay G, Al-Ansari T. A techno-economic-environmental study evaluating the potential of oxygen-steam biomass gasification for the generation of value-added products. Energy Convers Manag 2019;196:664–76. https://doi.org/10.1016/j.enconman.2019.06.019.

[51] Song H-S, Ramkrishna D, Trinh S, Wright H. Operating strategies for Fischer-Tropsch reactors: A model-directed study. Korean J Chem Eng 2004;21:308–17. https://doi.org/10.1007/BF02705414.

[52] Gangadharan P, Kanchi KC, Lou HH. Evaluation of the economic and environmental impact of combining dry reforming with steam reforming of methane. Chem Eng Res Des 2012;90:1956–68. https://doi.org/10.1016/j.cherd.2012.04.008.

[53] Lavoie J-M. Review on dry reforming of methane, a potentially more environmentally-friendly approach to the increasing natural gas exploitation. Front Chem 2014;2:81.

[54] Jiang Z, Liao X, Zhao Y. Comparative study of the dry reforming of methane on fluidised aerogel and xerogel Ni/Al 2 O 3 catalysts. Appl Petrochemical Res 2013;3:91–9.

[55] Wang W-C, Tao L. Bio-jet fuel conversion technologies. Renew Sustain Energy Rev 2016;53:801–22. https://doi.org/10.1016/j.rser.2015.09.016.

[56] Gong S, Shinozaki A, Shi M, Qian E. Hydrotreating of Jatropha Oil over Alumina Based Catalysts. Energy Fuel 2012;26:2394–9. https://doi.org/10.1021/ef300047a.

[57] Liu J, Liu C, Zhou G, Shen S, Rong L. Hydrotreatment of Jatropha oil over NiMoLa/Al2O3 catalyst. Green Chem 2012;14:2499–505. https://doi.org/10.1039/C2GC35450K.

[58] Liu J, Lei J, He J, Deng L, Wang L, Fan K, et al. Hydroprocessing of Jatropha Oil for Production of Green Diesel over Non-sulfided Ni-PTA/Al2O3 Catalyst. Sci Rep 2015;5:11327.

[59] Anand M, Farooqui SA, Kumar R, Joshi R, Kumar R, Sibi MG, et al. Optimizing renewable oil hydrocracking conditions for aviation bio-kerosene production. Fuel Process Technol 2016;151:50–8. https://doi.org/10.1016/j.fuproc.2016.05.028.

[60] Verma D, Kumar R, Rana BS, Sinha AK. Aviation fuel production from lipids by a single-step route using hierarchical mesoporous zeolites. Energy Environ Sci 2011;4:1667–71. https://doi.org/10.1039/C0EE00744G.

[61] Phillips S, Tarud J, Biddy M, Dutta A. Gasoline from Woody Biomass via Thermochemical Gasification, Methanol Synthesis, and Methanol-to-Gasoline Technologies: A Technoeconomic Analysis. Ind Eng Chem Res 2011:50. https://doi.org/10.1021/ie2010675.

[62] Diniz APMM, Sargeant R, Millar GJ. Stochastic techno-economic analysis of the production of aviation biofuel from oilseeds. Biotechnol Biofuels 2018;11:161. https://doi.org/10.1186/s13068-018-1158-0.

[63] Oblad AG, Shabtai J, Coppola EN. Improvement of jet fuel properties by paraffin isomerization. Am Chem Soc 1987:32.

[64] Dhar A, Vekariya RL, Sharma P. Kinetics and mechanistic study of n-alkane hydroisomerization reaction on Pt-doped γ-alumina catalyst. Petroleum 2017;3:489–95. https://doi.org/10.1016/j.petlm.2017.02.001.
[65] Jahangiri M, Salehirad F, Alijani S. Preparation of Pt/Al2O3-Cl Catalyst and Investigation of Operating Variables Effects on Isomerization Reaction. J Chem Pet Eng 2018;52:13–21. https://doi.org/10.22059/jchpe.2018.233982.1198.
[66] Tongpun P, Wang W-C, Srinophakun P. Techno-economic analysis of renewable aviation fuel production: From farming to refinery processes. J Clean Prod 2019;226:6–17. https://doi.org/10.1016/j.jclepro.2019.04.014.
[67] Roy S. Economics of Small Scale Jatropha Production for Biofuels in India. McGill University (Canada); 2011.
[68] Suriharn B, Sanitchon J, Songsri P, Kesmala T. Effects of Pruning Levels and Fertilizer Rates on Yield of Physic Nut (Jatropha Curcas L.). Asian J Plant Sci 2011;10:52–9.
[69] Neto O, Santos A, Folegatti MV, Lena BP, Diotto AV, Francisco JP, et al. Energy analysis of Jatropha curcas under irrigation and rainfed at the Southeast Brazilian humid subtropical. CIGR J 2018;20:116–26.
[70] Woqod. Qatar transportation fuel prices 2020. http://www.woqod.com/EN/Gas/Pages/Fuel-Price.aspx (accessed September 10, 2020).
[71] hampshiregenerators. Three Phase Diesel Generator 2021. https://www.hampshiregenerators.co.uk/product/generators/diesel-generators/inmesol-iv-220-200kva-160kw-three-phase-diesel-generator-400v/?gclid=CjwKCAiAlrSPBhBaEiwAuLSDULgi9QudZ2eYduioqv2fCQaU6mmLko8KQBOmJEG6oEiiNzJvYReKDxoCqlQQAvD_BwE (accessed May 21, 2021).
[72] Cotterillcivils. 50,000 litre Galvanised Steel Water Tank 2021. https://www.cotterillcivils.co.uk/shop/water-tanks/galvanised-steel/galvanised-steel-water-tank-50000-litre-bottom-outlet-anti-algae-cover/?gclid=CjwKCAiAlrSPBhBaEiwAuLSDUFWn61e2oF3OAktaD-9dJyu6YiudLaYxjScMvZj1il8TxCIzsHl-hhoCtVkQAvD_BwE (accessed May 21, 2021).
[73] Inverter. 10 hp Horizontal Centrifugal Pump 2021. https://www.inverter.com/10hp-horizontal-centrifugal-pump (accessed May 21, 2021).
[74] CheckTrade. Irrigation system cost 2021. https://www.checkatrade.com/blog/cost-guides/irrigation-system-cost/ (accessed April 21, 2021).
[75] DirectWaterTanks. Reconditioned IBC 2021. https://www.directwatertanks.co.uk/1000-litre-reconditioned-ibc-white-plastic-pallet-grade-1?gclid=CjwKCAiAlrSPBhBaEiwAuLSDUJTUfBTvubIc2AYWQdWeIIhb5Y38DdQK4lXRyUyEOddAdK0vzUy9xBoCk20QAvD_BwE (accessed May 21, 2021).
[76] Calpeda. Calpeda CTM61 Peripheral Booster Pump 2021. https://www.anchorpumps.com/calpeda-ctm61-peripheral-booster-pump-240v?gclid=CjwKCAiAlrSPBhBaEiwAuLSDUESiaTkq0Yoz0bo5Q3N7SFGkt2TBiv0c1X1E-QRGm6Wm3m7VCdUxyRoCpDUQAvD_BwE (accessed May 21, 2021).
[77] Indiamart. Galvanized Steel Shipping Storage Container 2021. https://www.indiamart.com/proddetail/used-shipping-storage-container-11022255491.html (accessed November 20, 2021).
[78] A. Phocaides. Technical handbook on pressurized irrigation techniques. Rome: 2000.
[79] Bazaraa AS. Estimates of potential evapotranspiration over the State of Qatar. Eng J Qatar Univ 1989:2.
[80] Garg KK, Wani SP, Rao AVRK. Crop coefficients of Jatropha (Jatropha curcas) and Pongamia (Pongamia pinnata) using water balance approach. Wiley Interdiscip Rev Energy Environ 2014;3:301–9. https://doi.org/10.1002/wene.88.
[81] Lena BP, Folegatti MV, Flumignan DL, Irmak S, Francisco JP, Diotto AV, et al. Water Requirement and Crop Coefficients of Young Jatropha curcas L. Trees in a Subtropical Humid Environment. J Irrig Drain Eng 2021;147:4021020.
[82] Gulftimes. Ashghal sets fee for services 2020. https://www.gulf-times.com/story/653326/Ashghal-sets-fee-for-services (accessed August 13, 2020).
[83] Bandara J, Senanayake N, Abeyweera R. A Renewable Energy based Power Supply System for Water Pumping and Lighting in a Rural Village. SLEMA J 2015;18:1–11.
[84] SalaryExplorer. Average Salary in Qatar 2021. http://www.salaryexplorer.com/salary-survey.php?loc=176&loctype=1 (accessed October 10, 2021).
[85] ChemEngOnline. Chemical Engineering Plant Cost Index (CEPCI) n.d. https://www.chemengonline.com/pci-home (accessed January 1, 2020).
[86] S&Pglobal. Global Hydrogen Price Assessment 2019. https://www.spglobal.com/platts/en/our-methodology/price-assessments/energy-transition/hydrogen-price-assessments (accessed January 10, 2022).
[87] Cynthia O-B, Keat TL. Feasibility of Jatropha Oil for Biodiesel: Economic Analysis 2011. https://doi.org/10.3384/ecp11057463.
[88] Zhu Y, Albrecht KO, Elliott DC, Hallen RT, Jones SB. Development of hydrothermal liquefaction and upgrading technologies for lipid-extracted algae conversion to liquid fuels. Algal Res 2013;2:455–64. https://doi.org/10.1016/j.algal.2013.07.003.
[89] KaiDa. Platinum catalysts price 2019. http://www.kaida.co.uk/pt_catalysts.html (accessed December 6, 2020).
[90] Neuling U, Kaltschmitt M. Techno-economic and environmental analysis of aviation biofuels. Fuel Process Technol 2018;171:54–69. https://doi.org/10.1016/j.fuproc.2017.09.022.
[91] Indiamart. Carbon dioxide gas price. 2021.
[92] IEA. Global fuel price changes, 2005-2019 2020. https://www.iea.org/data-and-statistics/charts/global-fuel-price-changes-2005-2019 (accessed January 5, 2022).
[93] National Energy Technology Laboratory. Baseline Technical and Economic Assessment of a Commercial Scale Fischer-Tropsch Liquids Facility. 2007.
[94] Franziska Müller-Langer. Analyse und Bewertung ausgewählter zukünftiger Biokraftstoffoptionen auf der Basis fester Biomasse. 2011.
[95] Max SP, Klaus DT, Ronald EW. Plant design and economics for chemical engineers. McGraw-Hill Companies; 2003.
[96] Kristina M. Holmgren. Investment cost estimates for gasificationbased biofuel production systems. 2015.
[97] Zhu Y, Biddy MJ, Jones SB, Elliott DC, Schmidt AJ. Techno-economic analysis of liquid fuel production from woody biomass via hydrothermal liquefaction (HTL) and upgrading. Appl Energy 2014;129:384–94. https://doi.org/10.1016/j.apenergy.2014.03.053.
[98] Wright MM, Daugaard DE, Satrio JA, Brown RC. Techno-economic analysis of biomass fast pyrolysis to transportation fuels. Fuel 2010;89:S2–.
[99] Peters MS, Timmerhaus KD, West RE. Plant design and economics for chemical engineers. vol. 4. McGraw-Hill New York; 2003.
[100] International Energy Agency. Projected Costs of Generating Electricity. Paris: OECD/ IEA/NEA; 2010.
[101] IPCC. 5th Assessment on Climate Change. 2014.
[102] Winnipeg. Emission factors in kg CO2-equivalent per unit 2012. https://winnipeg.ca/finance/findata/matmgt/documents//2012/682-2012//682-2012_Appendix_H-WSTP_South_End_Plant_Process_Selection_Report/Appendix 7.pdf (accessed December 25, 2019).
[103] Lokesh K, Sethi V, Nikolaidis T, Goodger E, Nalianda D. Life cycle greenhouse gas analysis of biojet fuels with a technical investigation into their impact on jet engine performance. Biomass Bioenergy 2015;77:26–44. https://doi.org/10.1016/j.biombioe.2015.03.005.
[104] Kumar S, Chaube A, Jain SK. Sustainability issues for promotion of Jatropha biodiesel in Indian scenario: A review. Renew Sustain Energy Rev 2012;16:1089–98. https://doi.org/10.1016/j.rser.2011.11.014.
[105] Doe. Refinery siting workbook: appendices A and B. United States 1980. https://doi.org/10.2172/5146479.
[106] European Commission. Energy use in buildings 2020. https://ec.europa.eu/energy/eu-buildings-factsheets-topics-tree/energy-use-buildings_en (accessed October 1, 2020).
[107] Klufallah MMA, Nuruddin MF, Khamidi MF, Jamaludin N. Assessment of carbon emission reduction for buildings projects in Malaysia-A comparative analysis. E3S Web Conf., vol. 3, EDP Sciences; 2014, p. 1016.
[108] Beeson R. The Rail Central Rail Freight Interchange. 2018.
[109] BEIS. H2 emissions potential literature review. 2019.
[110] Chen Z, Shen Q, Sun N, Wei W. Life cycle assessment of typical methanol production routes: The environmental impacts analysis and power optimization. J Clean Prod 2019;220:408–16. https://doi.org/10.1016/j.jclepro.2019.02.101.
[111] Soltani R, Rosen MA, Dincer I. Assessment of CO2 capture options from various points in steam methane reforming for hydrogen production. Int J Hydrogen Energy 2014;39:20266–75. https://doi.org/10.1016/j.ijhydene.2014.09.161.
[112] Wei H, Liu W, Chen X, Yang Q, Li J, Chen H. Renewable bio-jet fuel production for aviation: A review. Fuel 2019;254:115599. https://doi.org/10.1016/j.fuel.2019.06.007.
[113] D-Waste. Landfill volume calculator 2022. http://www.landvol.d-waste.com/calc.html (accessed January 15, 2022).
[114] Sun H, Park Y. CO2 Emission Calculation Method during Construction Process for Developing BIM-Based Performance Evaluation System. Appl Sci 2020;10:5587. https://doi.org/10.3390/app10165587.
[115] Manure Management 2018. accessed March 20, 2021, http://www.fao.org/faostat/en/#data/GM/visualize.
[116] Scclmines. Environmental Standards 2022. https://scclmines.com/env/Linkfile2.htm (accessed January 15, 2022).
[117] DOE UD of E. Alternative Aviation Fuels: Overview of Challenges, Opportunities, and Next Steps. 2016.
[118] Harden CJ. Discount rate development in oil and gas valuation. OnePetro: SPE Hydrocarb. Econ. Eval. Symp; 2014.
[119] ICAO. CORSIA Sustainability Criteria for CORSIA Eligible Fuels. 2021.
[120] RSB - Roundtable on Sustainable Biomaterials. RSB Standard for ICAO CORSIA. Geneva: 2021.